AD NUMBER
AD855565
LIMITATION CHANGES
TO: **Approved for public release; distribution is unlimited.**
FROM: **Distribution authorized to U.S. Gov't. agencies and their contractors; Critical Technology; JUN 1969. Other requests shall be referred to Air Force Weapons Laboratory, Kirtland AFB, NM 87117. This document contains export-controlled technical data.**
AUTHORITY
AFWL ltr, 30 Nov 1971

AFWL-TR-
68-146

A CURVED FLYER PLATE TECHNIQUE FOR IMPULSIVE LOADING OF RINGS AND A PASSIVE IMPULSE GAGE FOR UNDERGROUND NUCLEAR TESTS

Alexander L. Florence

Poulter Laboratory for High Pressure Research
Stanford Research Institute
Menlo Park, California

Contract F29601-67-C-0105

TECHNICAL REPORT NO. AFWL-TR-68-146

June 1969

AIR FORCE WEAPONS LABORATORY
Air Force Systems Command
Kirtland Air Force Base
New Mexico

BLANK PAGE

AFWL-TR-68-146

AIR FORCE WEAPONS LABORATORY
Air Force Systems Command
Kirtland Air Force Base
New Mexico

When U. S. Government drawings, specifications, or other data are used for any purpose other than a definitely related Government procurement operation, the Government thereby incurs no responsibility nor any obligation whatsoever, and the fact that the Government may have formulated, furnished, or in any way supplied the said drawings, specifications, or other data, is not to be regarded by implication or otherwise, as in any manner licensing the holder or any other person or corporation, or conveying any rights or permission to manufacture, use, or sell any patented invention that may in any way be related thereto.

This report is made available for study with the understanding that proprietary interests in and relating thereto will not be impaired. In case of apparent conflict or any other questions between the Government's rights and those of others, notify the Judge Advocate, Air Force Systems Command, Andrews Air Force Base, Washington, D. C. 20331.

DO NOT RETURN THIS COPY. RETAIN OR DESTROY.

AFWL-TR-68-146

A CURVED FLYER PLATE TECHNIQUE FOR IMPULSIVE LOADING OF RINGS AND A PASSIVE IMPULSE GAGE FOR UNDERGROUND NUCLEAR TESTS

Alexander L. Florence

Poulter Laboratory for High Pressure Research
Stanford Research Institute
Menlo Park, California
Contract F29601-67-C-0105

TECHNICAL REPORT NO. AFWL-TR-68-146

FOREWORD

This report was prepared by Poulter Laboratory for High Pressure Research, Stanford Research Institute, Menlo Park, California, under Contract F29601-67-C-0105. The research was performed under Program Element 6.16.46.01.H, Project 5710, Subtask 01.028, and was funded by the Defense Atomic Support Agency (DASA).

Inclusive dates of research were July 1968 to January 1969. The report was submitted 22 April 1969 by the Air Force Weapons Laboratory Project Officer, Lt Ronald Schappaugh (WLRP).

The Contractor's account reference number is SRI Project PGU-6852.

The author is indebted to L. J. Dary for carrying out the experimental program for the development of the curved flyer plate simulation technique, to K. E. Nelson for operating the X-ray camera, to W. A. Zietzke for carrying out the experimental program for the development of the passive impulse gage and for contributing the ideas essential to its operation. The author is also indebted to G. R. Abrahamson and H. E. Lindberg for valuable discussions during the course of the program.

In the course of performing the experiments commercial products were used which can be described only by using their trade names because their physical and chemical description and method of manufacture are proprietary information. These products are Detasheet D, Epon 934 and Thornel 25. Permission for the use of these trade names has been obtained from the manufacturers.

Information in this report is embargoed under the U.S. Export Control Act of 1949, administered by the Department of Commerce. This report may be released by departments or agencies of the U.S. Government to departments or agencies of foreign governments with which the United States has defense treaty commitments, subject to approval of AFWL (WLRP).

This technical report has been reviewed and is approved.

RONALD D. SCHAPPAUGH
Lt, USAF
Project Officer

HARRY F. RIZZO
Lt Colonel, USAF
Chief, Physics Branch

CLAUDE K. STAMBAUGH
Colonel, USAF
Chief, Research Division

ABSTRACT

(Distribution Limitation Statement No. 2)

A technique has been developed for impulsive loading of rings. It consists of spalling a thin, curved flyer plate from the inner surface of a curved buffer plate by the pressure pulse from sheet explosive on an outer surface. The flyer plate travels radially inward a short distance before impacting a test ring. A $\cos \theta$ ($-\pi/2 < \theta < \pi/2$) circumferential distribution of impulse is achieved by an appropriate circumferential variation in buffer thickness. The technique is suitable for peak impulses up to 8000 taps. (Above this impulse level sheet explosive in direct contact with test rings provides the required simulation.) Impulse calibration data is presented for 25-mil and 50-mil-thick flyer plates of 6061-T6 aluminum. Tests indicate that the technique is suitable for aboveground screening of hardened materials.

A passive impulse gage has been developed for use in underground nuclear tests. It consists of a piston and restraining spring and incorporates a recording device for separating the piston deflection due to the impulsive load and the deflection due to later arriving extraneous loads.

This page intentionally left blank.

CONTENTS

ILLUSTRATIONS

ILLUSTRATIONS (Concluded)

TABLES

SECTION I

INTRODUCTION

This report describes research and development in two areas: (1) a curved flyer plate technique for impulsive loading of rings, and (2) passive impulse gages. Both areas are in direct support of underground nuclear tests.

The curved flyer plate technique described in Section II was developed to provide combined shock and structural response of ring models representing slices of reentry vehicle structures. The maximum peak impulses obtainable with 25-mil and 50-mil-thick flyers of 1100-0 aluminum are about 5000 and 8000 taps. Above these impulse levels, sheet explosive can be used in direct contact with rings; flyer plates projected by sheet explosive in direct contact or projected electromagnetically can also be used. A circumferential distribution of impulse over one side of a ring varying approximately as $\cos \theta$ $(-\pi/2 < \theta < \pi/2)$ is readily provided by this technique. Tests on rings described in Section II indicate that the curved flyer plate technique is valuable for aboveground screening of hardened materials.

A passive impulse gage, consisting of a simple spring-mass system, was developed to measure impulses encountered in underground nuclear tests. The gage, described in Section III, promises to be superior in performance to existing passive impulse gages and incorporates a recording device for separating piston deflections caused by impulses from those caused by later extraneous loads such as "hurricanes," ground motion, and bulkhead shock.

This page intentionally left blank.

SECTION II

A CURVED FLYER PLATE TECHNIQUE FOR IMPULSIVE LOADING OF RINGS

1. INTRODUCTION

A nuclear explosion can impulsively load the exposed surface of a nearby reentry vehicle (RV). For several years this impulsive loading has been simulated by loading from sheet explosives and by loading from impacts with flat flyer plates. Simulation with explosives has been used primarily to obtain structural responses of RV structural components, the main component being essentially a cylindrical shell. Simulation with flat flyer plates has been used to obtain material or stress-wave responses, such as spall, in small, flat samples representing elements of an RV wall. An electromagnetic technique* is now being used to project curved flyer plates at rings and cylinders to obtain combined material and structural responses. Combined response can also be produced by application of sheet explosive in direct contact with the vehicle surface, but strip loading is necessary for impulses less than 6000 taps.**

The technique described in this report is a modification of a technique reported in Ref. 1; the development thus takes advantage of this earlier research. A thin, semicircular flyer plate is "spalled" from the inside surface of a thick, semicircular buffer plate by a pressure pulse from sheet explosive† on the outside surface of the buffer plate, the detonation front traveling around the circumference. The flyer plate then impacts half the circumference of a test ring located within the

---

*Developed by EG&G, Bedford, Massachusetts.

**1 tap ≡ 1 dyne-sec/cm^2.

†Detasheet, manufactured by Du Pont.

arc of the buffer plate, providing the required short-duration pressure pulse. Short-duration pressure pulses can be obtained much more easily from sheet explosive placed in direct contact with the test material. However, if in addition to a short pulse a low impulse is required, the flyer plate technique has a major advantage. This is because sheet explosive currently in use detonates reliably only when thicknesses exceed 10 to 12 mils, a thickness that corresponds to an impulse of about 6000 taps. For lower impulses, strips of 12-mil-thick sheet explosive are spaced to result in an average thickness of less than 12 mils. This method, although it may still be suitable for structural response investigations, gives appropriate stress wave response only beyond a depth at which the pressure fluctuation between strips is acceptable. The nonuniformity of the stress wave pattern can be minimized by using a suitable attenuator between the sheet explosive strips and the sample, but the attenuator has the undesirable effect of increasing the duration of the pressure pulse.

The curved flyer plate technique described below provides short pressure pulses with low impulses and is designed specifically for loading rings, although application to cylindrical shells is possible. Furthermore, the impulse over the loaded half of the test ring varies as $\cos\theta$, where $-\pi/2 < \theta < \pi/2$, θ being the angular coordinate from the plane of symmetry. One simplification embodied in this technique is that it makes use of a supersonic running impact of flyer and target instead of the usual simultaneous impact. Justification of the use of running impact for stress wave response in materials is included in current research at Stanford Research Institute (SRI).*

2. DESCRIPTION OF THE CURVED FLYER PLATE TECHNIQUE

Figure 1 shows schematically an experimental setup that was designed for impulsively loading rings 6 inches in diameter and 1 inch

*Contract F29601-67-C-0075 between the Air Force Weapons Laboratory (AFWL) and SRI.

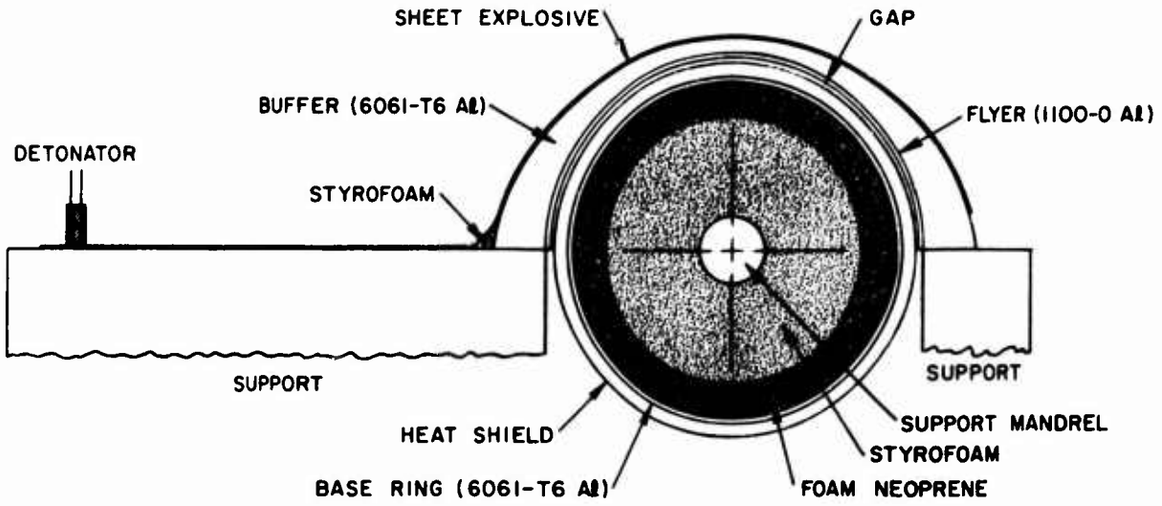

(a) SIDE VIEW

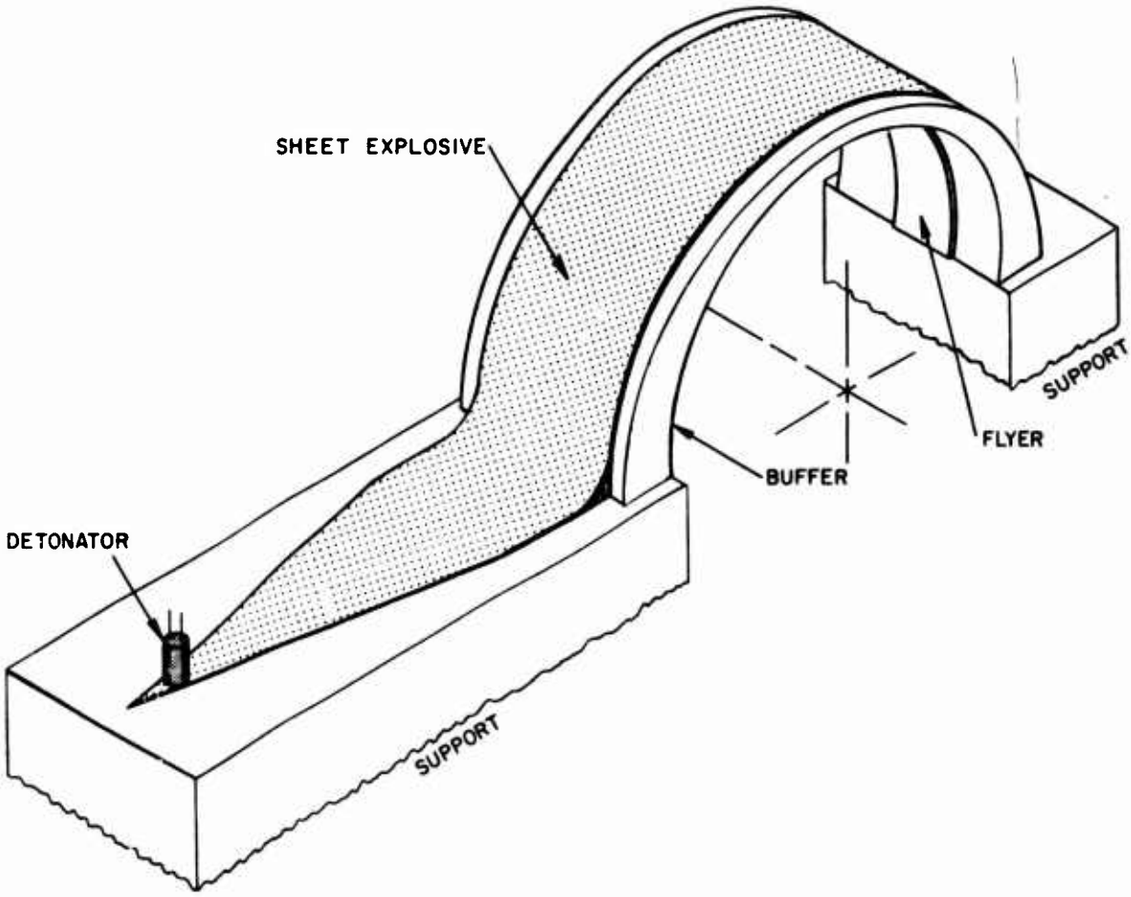

(b) ISOMETRIC VIEW WITH TEST RING REMOVED

GB-6852-34

FIG. 1 EXPERIMENTAL ARRANGEMENT FOR FLYER PLATE TECHNIQUE

wide. Figures 2 through 4 show the experimental setup. Figure 2 shows the complete setup ready for firing. Figure 3 shows the setup with the explosive, buffer plate, and flyer plate removed, and Fig. 4 shows the test ring and buffer-flyer assembly. Shown in Figs. 2 and 3, but omitted from Fig. 1, are two steel arches fitted within the buffer plates. These steel arches serve to reduce the inward motion of the buffer plates.

A semicircular flyer plate is rolled from a flat, 1-inch-wide strip of 1100-O Aluminum to the inside diameter of the buffer plate and held firmly in place by clamps at each end (Fig. 4). The contact surfaces were coated with SAE 30 motor oil before being brought together to eliminate air pockets; this allows a more uniform passage of stress waves across the flyer-buffer interface. (Flyer plate thicknesses of 25 and 50 mils were used in the technique development.)

The buffer plate of 6061-T6 aluminum alloy is machined from standard tubing by two circular arcs so that it has a plane of symmetry and has its thinnest section in the middle. The variable buffer thickness is designed to provide a cosine distribution of flyer plate velocity, its maximum being at the center.

As shown in Figs. 1 and 2, sheet explosive is placed around the outside of the buffer plate. The lead-in portion of the explosive approaches the buffer plate from a radial direction so that, upon detonation, the detonation front travels around the circumference of the buffer plate. The resulting development of the stress waves is complicated, but basically a compressive stress pulse emanates from the detonation front, passes through the buffer and flyer plates, and reflects from the free inner surface of the flyer plate to form a tensile stress pulse. Upon arrival of this tensile stress pulse at the buffer-flyer interface, separation occurs and the flyer plate is thus launched.

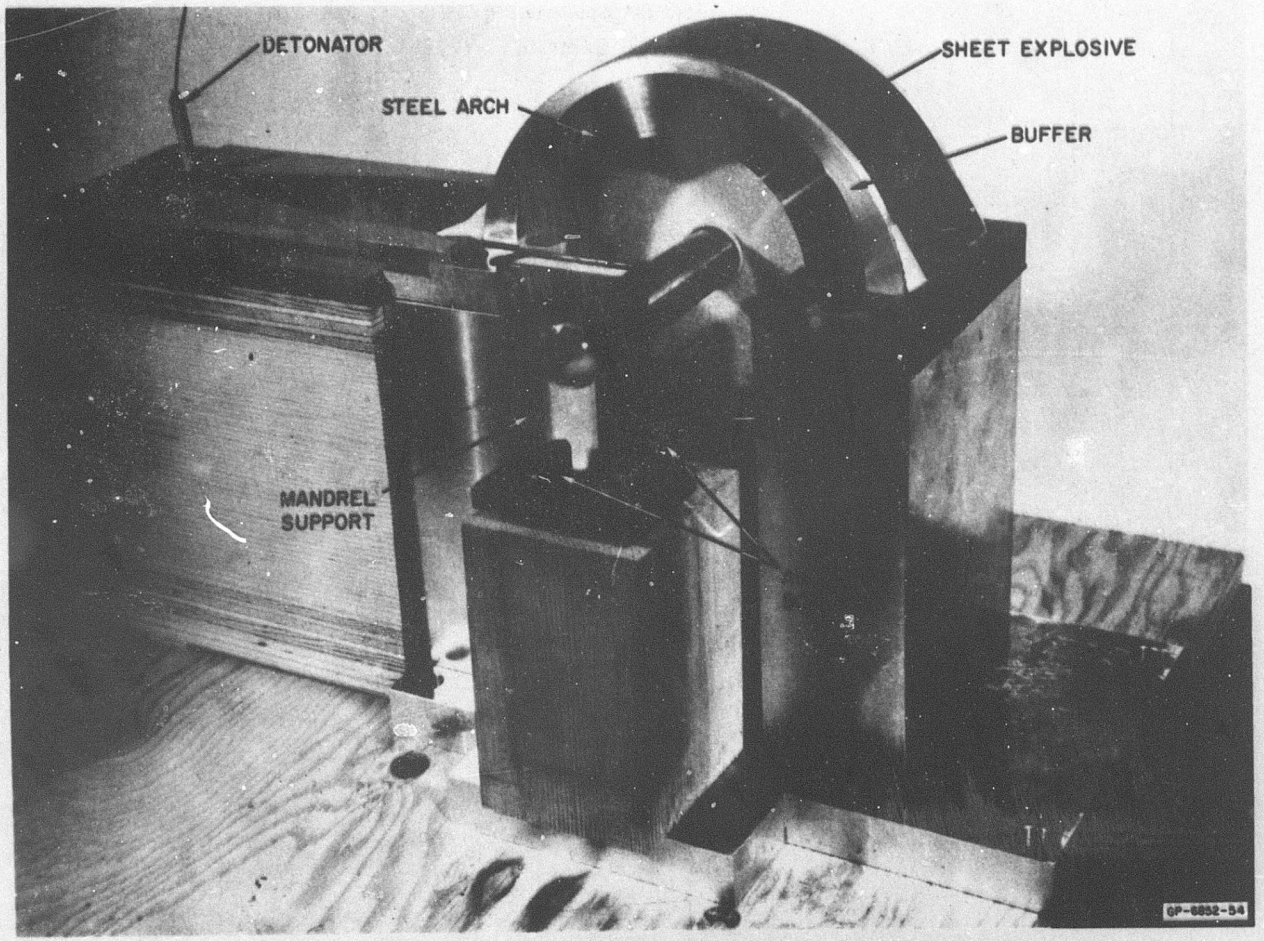

FIG. 2 EXPERIMENTAL ARRANGEMENT FOR FLYER PLATE TECHNIQUE

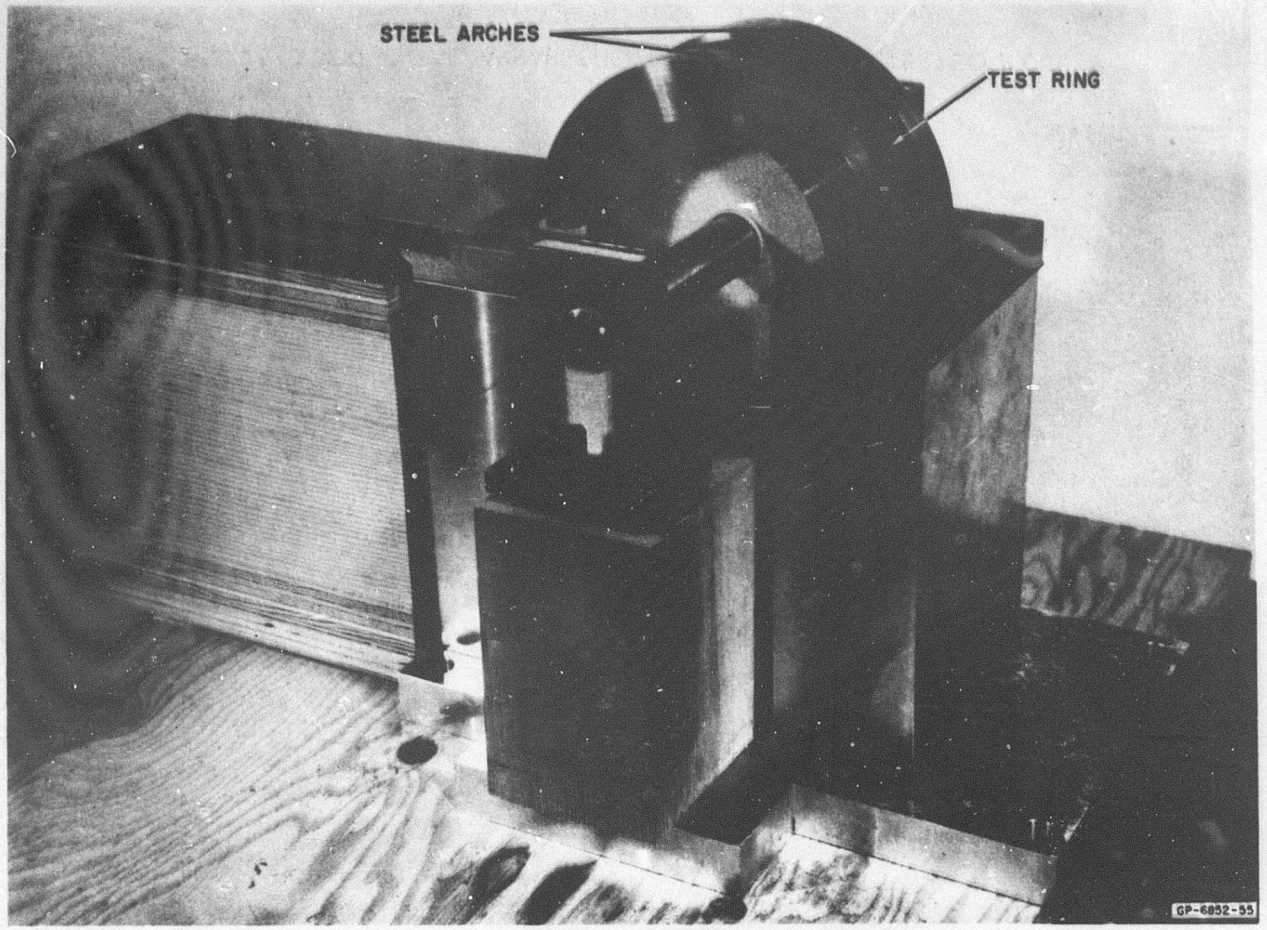

FIG. 3 EXPERIMENTAL ARRANGEMENT FOR FLYER PLATE TECHNIQUE
(sheet explosive, buffer, and flyer plates removed)

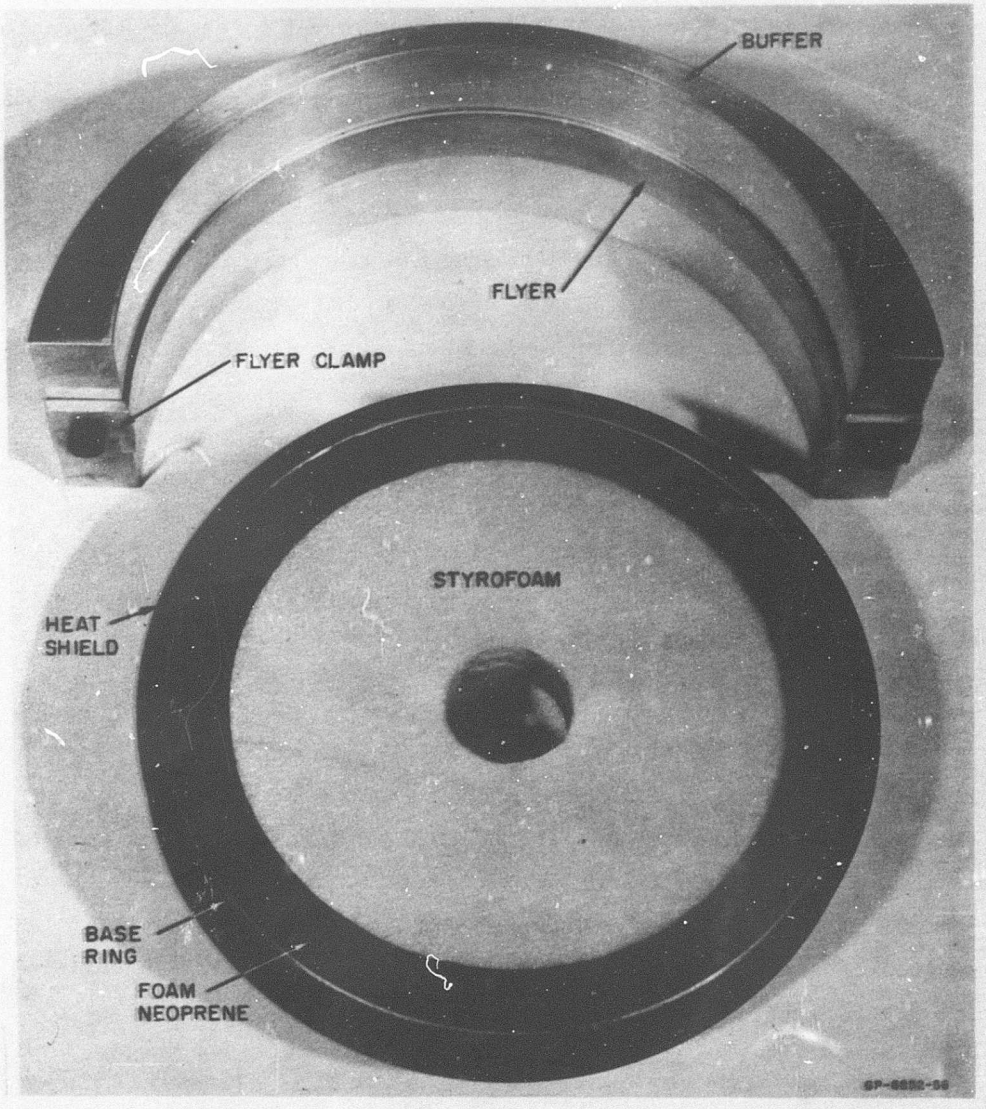

FIG. 4 BUFFER-FLYER ASSEMBLY—TEST RING WITH SUPPORT METHOD

Because the incident stress pulse is attenuated as it proceeds through the plates, the shape of the reflected pulse depends upon the combined thickness of the plates. Consequently the momentum trapped by the flyer plate depends upon the combined thickness. Thus the distribution of flyer plate velocity around the circumference can be controlled by the variation of buffer plate thickness. Calibration

experiments, described in Section II.3c, were performed to obtain the relationship among thicknesses of sheet explosive, buffer and flyer plates, and the flyer plate velocity. From these results the peak impulse and distribution were determined.

As mentioned previously the above method of launching a flyer plate provides an impact that travels around the test ring at a velocity close to the detonation velocity of the explosive and obviates the difficulties of providing a simultaneous impact.

3. DESIGN OF THE CURVED FLYER PLATE TECHNIQUE

The design and development of the technique were primarily experimental but guided by simple theoretical concepts. Most of the basic experimental investigation was carried out with flat sheet explosive, and buffer and flyer plates, and the results were assumed valid for explosives and plates in a curved configuration. The investigation is now described.

a. Flyer Plates

When a curved flyer plate is projected radially inwards toward a target ring it forms an arc of smaller radius, and circumferential compressive stresses are set up which for sufficient travel cause the plate to buckle. Figure 5 is a radiograph displaying such instability in a 25-mil-thick flyer plate spalled from the inner surface of a uniform buffer plate 1/2 inch thick. However, the buckles are imperceptible for small decreases in radii, e.g., 1/10 inch in a flyer plate of 3-inch radius. In view of this instability it was decided to employ 1100-0 Aluminum which has a low yield stress and flows to adapt to its new dimensions. Also this low yield stress does not allow significant slowing down of the plate before impacting the test ring due to a buildup of circumferential membrane forces. This material has a reasonably high mechanical impedance so that the pressures generated upon impact with low impedance heat shield materials, such as carbon phenolic and silica phenolic, do not differ greatly from the pressures generated by other suitable flyer plate materials impacting at the same velocity.

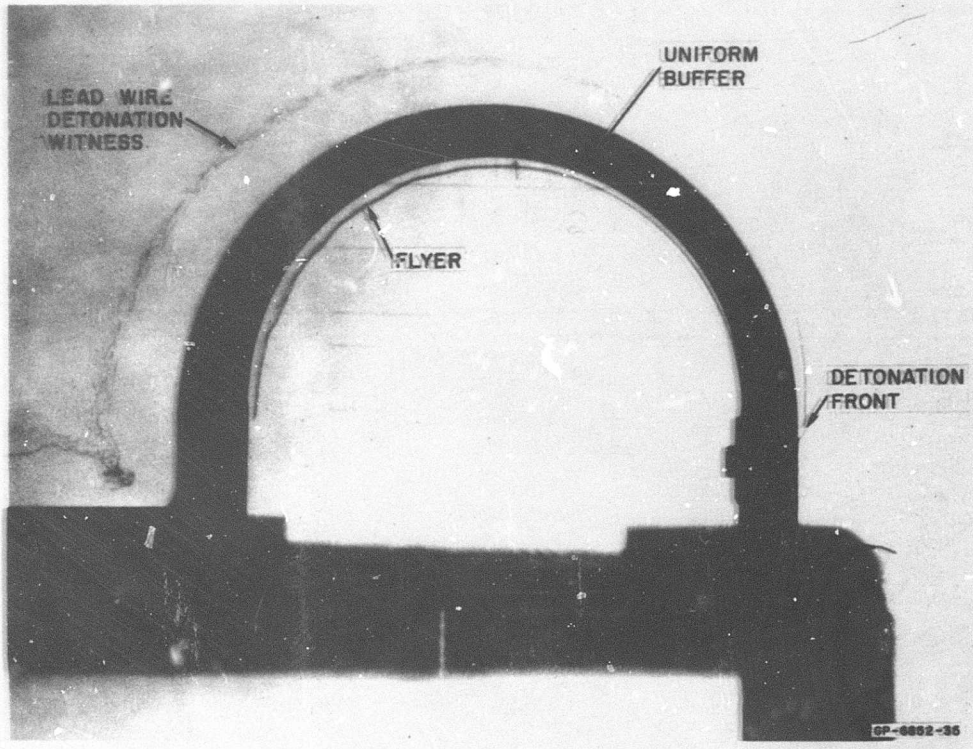

FIG. 5 RADIOGRAPH SHOWING FLYER PLATE INSTABILITY

b. Buffer Plates

To choose a buffer plate material a simple series of experiments was performed using the setup shown in Figs. 6 through 8. Aluminum flyer plates 6 inches long, 1 inch wide, and 12 mils thick were spalled from the lower surfaces of buffer plates, 9-1/2 inches long, 3 inches wide, and 1/2 inch thick by sheet explosive 2-1/2 inches wide and 20 mils thick. By the method described in Section II.3c, the flyer plate velocities were measured for buffer plates of three common metals, 6061-T6 Aluminum alloy, 1018 cold rolled steel, and brass alloy 356 (quarter hard leaded brass). From two tests with each buffer material the average velocities were respectively 0.124, 0.078, and 0.058 mm/μsec, results that give an indication of efficiency of impulse transfer from sheet explosive to momentum of flyer plate. Thus 6061-T6 Aluminum was chosen for the buffer material.

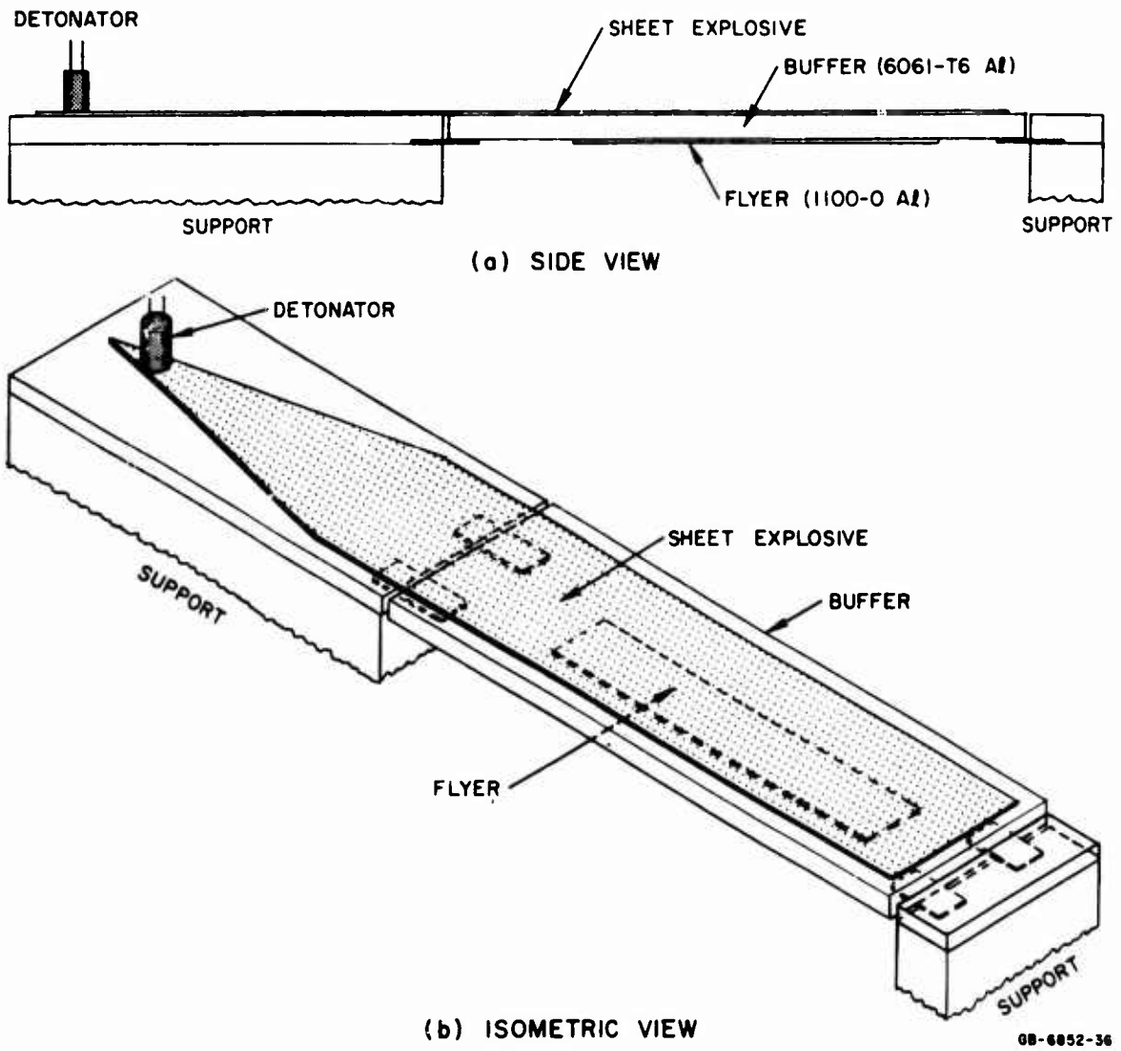

FIG. 6 EXPERIMENTAL ARRANGEMENT FOR IMPULSE CALIBRATION

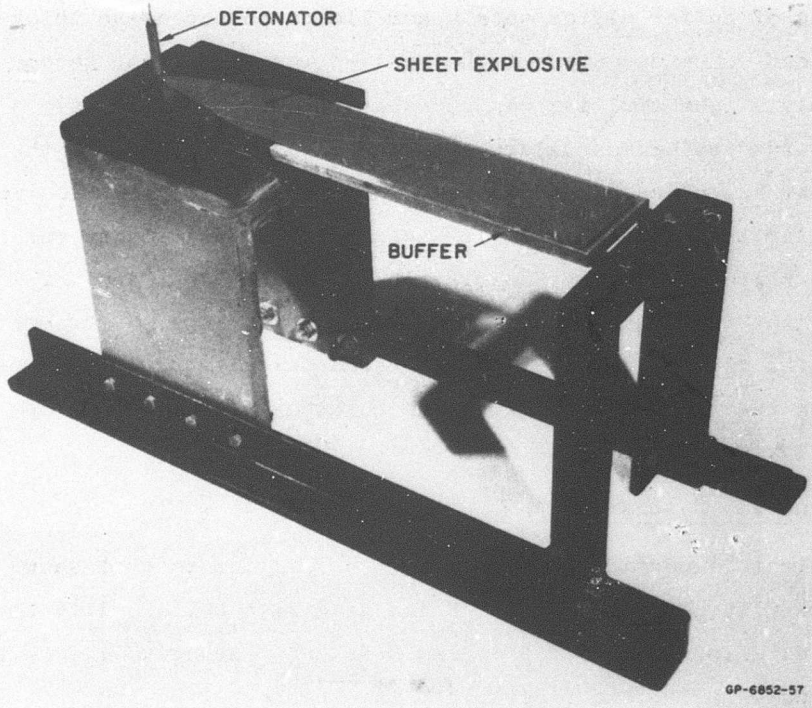

FIG. 7 EXPERIMENTAL ARRANGEMENT FOR IMPULSE CALIBRATION VIEWED FROM ABOVE

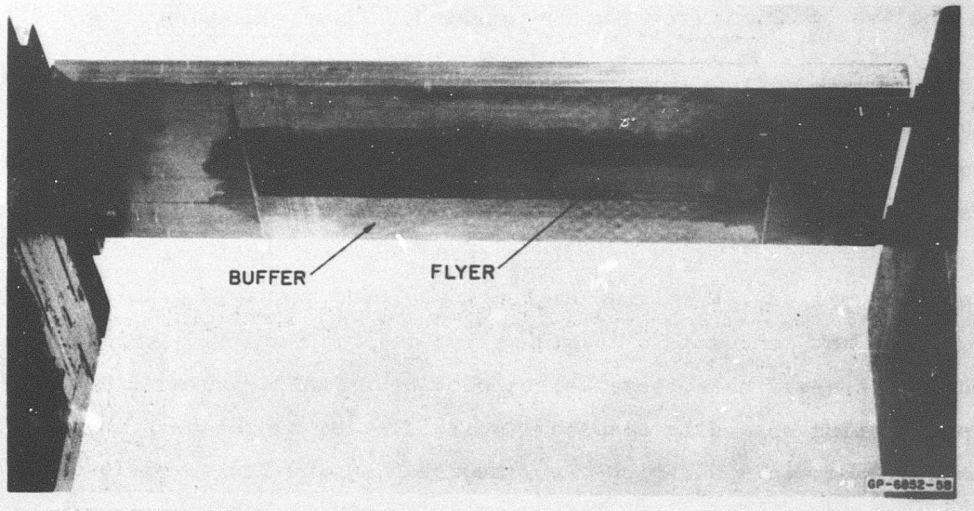

FIG. 8 EXPERIMENTAL ARRANGEMENT FOR IMPULSE CALIBRATION VIEWED FROM BELOW

Spalling of buffer plates sets upper limits on explosive thicknesses that can be used. Even if the spalled layer does not become detached, only slight spalling can be tolerated in order to avoid radially inward displacements large enough to cause impact with the test ring that has already been impacted by the flyer plate. To find these upper limits of sheet explosive thicknesses, spall tests were performed on buffer plates of 6061-T6 Aluminum, 1/4, 3/8, and 1/2 inch thick, with the experimental configuration shown in Figs. 6 through 8 but without the flyer plate. For these three thicknesses it was found that spalling was tolerable at explosive thicknesses of 25, 30, and 40 mils respectively.

c. Impulse Calibration

To calibrate experimental configurations similar to that shown in Fig. 1 the flat geometry of Fig. 6 was used with buffer plate thicknesses of 1/4, 5/16, 3/8, 1/2, 5/8, and 3/4 inch, explosive thicknesses of 25, 30, and 40 mils, and flyer plate thicknesses of 25 and 50 mils. Each assembly was placed in front of a flash X-ray camera, and shortly after the flyer had been launched a radiograph was taken. Figure 9 is a radiograph for the case of 30-mil-thick explosive, 3/8-inch-thick buffer, and 25-mil-thick flyer. Figure 10 shows how flyer plate velocities are obtained from the radiographs. First the slope $\tan \alpha = Y/X$ of the flyer plate is found. Then, with v and V denoting the flyer plate and detonation velocities, it follows from the

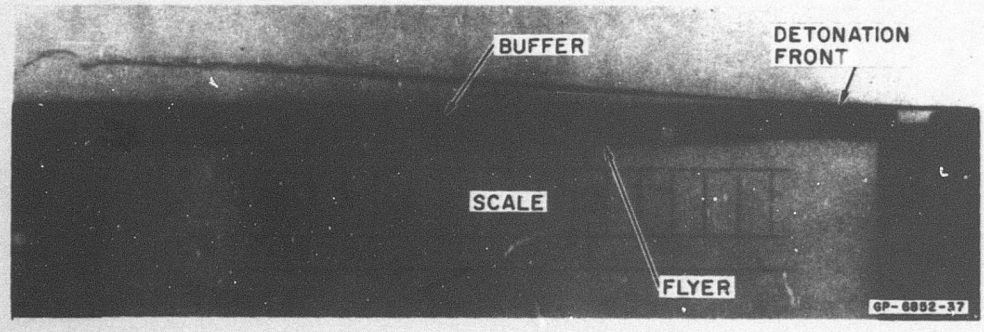

FIG. 9 RADIOGRAPH FOR DETERMINING FLYER VELOCITY

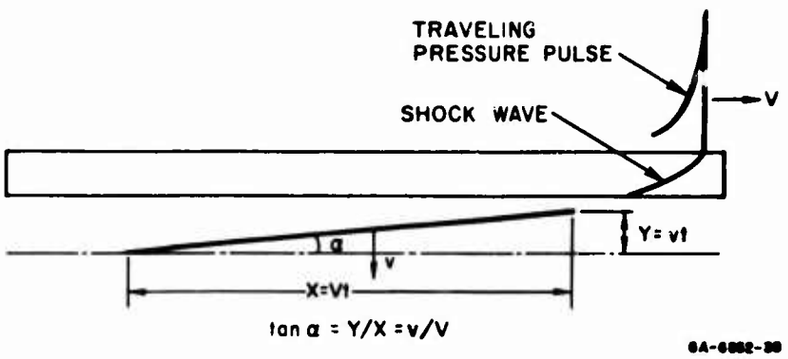

FIG. 10 GEOMETRY FOR CALCULATING FLYER VELOCITY

relations $Y = vt$ and $X = Vt$, where t is the time taken for the detonation front to traverse the flyer plate, that $v = V \tan \alpha$. The detonation velocity V for the sheet explosive is 7.2 mm/μsec.

Figures 11 and 12 give the results of the velocity calibration experiments. Figure 11 gives impulse versus buffer plate thickness for 25-mil-thick flyers, and Fig. 12 for 50-mil-thick flyers. Impulse signifies the flyer momentum, being the product of its velocity and its mass per unit area; the impulse values are applicable to targets that essentially bring flyer plates to rest (that is, targets of lower mechanical impedance which are much thicker than flyers). The points on the graphs represent averages of two, three, or four shots, as marked, and the curves fitted to these averages are recommended for use in the design of experiments. Figures 11 and 12 indicate that the maximum practical peak impulses associated with 25-mil-thick and 50-mil-thick flyers are about 5000 and 8000 taps. Impulses of 6000 taps and greater can be obtained with sheet explosive placed in direct contact with the target material, as discussed earlier.

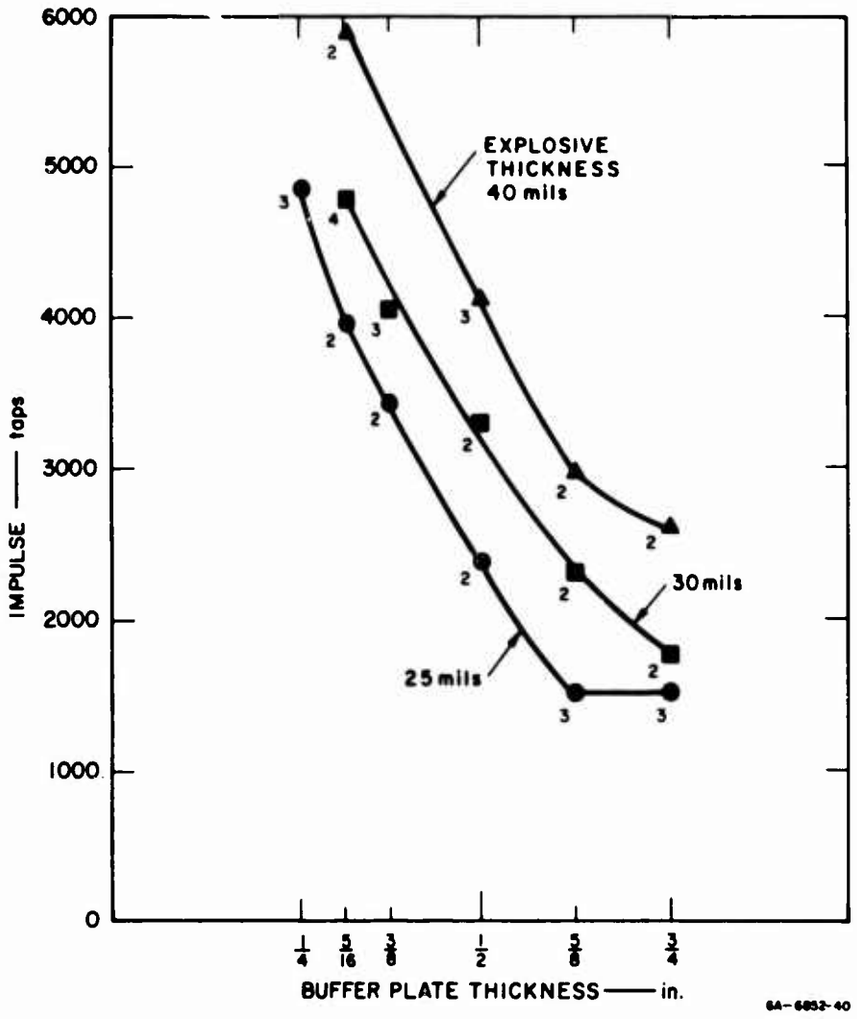

FIG. 11 CALIBRATION CURVES FOR 25-MIL-THICK FLYERS GIVING RELATIONSHIP AMONG IMPULSE, BUFFER THICKNESS, AND SHEET EXPLOSIVE THICKNESS

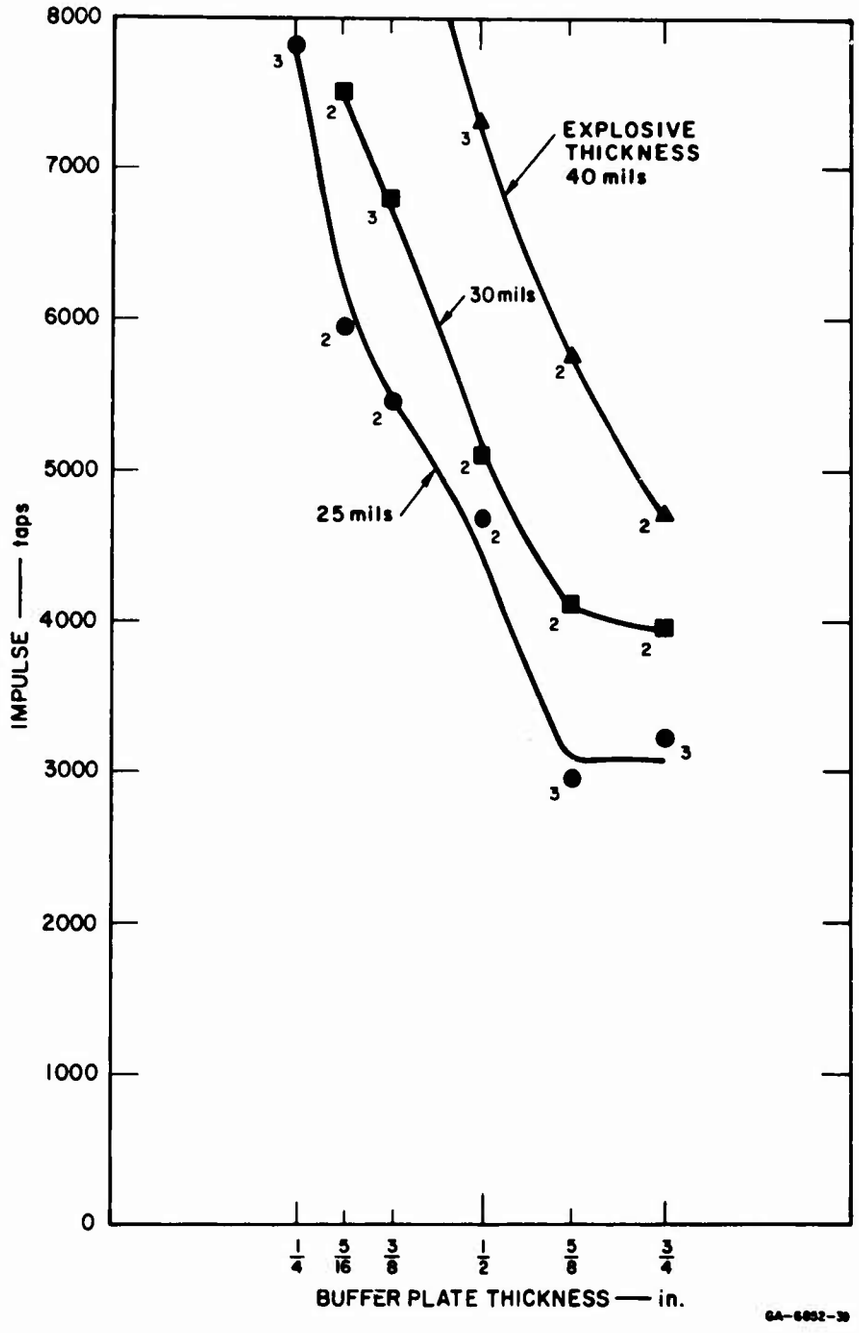

FIG. 12 CALIBRATION CURVES FOR 50-MIL-THICK FLYERS GIVING RELATIONSHIP AMONG IMPULSE, BUFFER THICKNESS, AND SHEET EXPLOSIVE THICKNESS

d. Velocity Distribution and Buffer Shape

Because a new buffer plate is required for every ring test it is desirable to exercise economy in buffer plate manufacture. This can be best achieved by machining the plate by two circular arcs as shown in Fig. 13. With a uniform layer of sheet explosive on the outside arc, it must still be determined if it is possible to obtain a distribution of radial velocity (or impulse) of a flyer plate on the inside arc varying approximately as cos θ around the circumference.

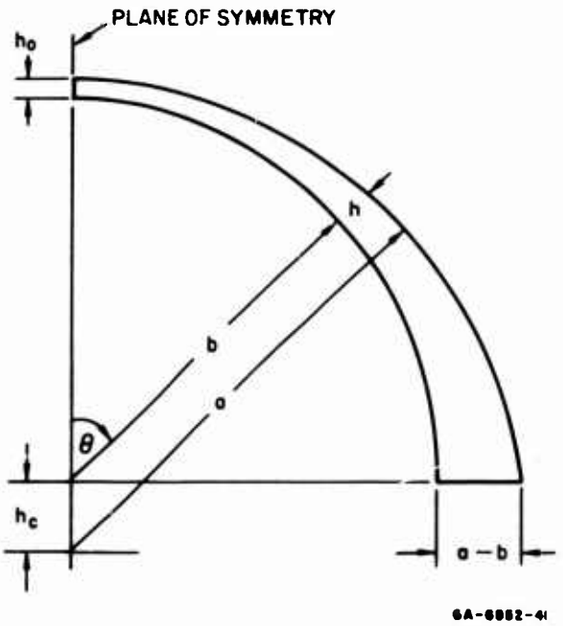

FIG. 13 BUFFER GEOMETRY

From the buffer plate geometry shown in Fig. 13 it can be established that the thickness h at any coordinate angle θ $(-\pi/2 \leq \theta \leq \pi/2)$ is

$$h = \left[a^2 - (h_c \sin \theta)^2 \right]^{1/2} - (b + h_c \cos \theta)$$

where a and b are the outer and inner radii and h_c is the distance between centers. This distance is calculated from $h_c = a - b - h_0$, where h_0 is the minimum thickness at $\theta = 0$. Calibration curves in Figs. 11 and 12 give impulse as a function of buffer thickness h, so

for specified thicknesses of explosive and flyer plate the distribution of impulse around the circumference is determined.

Three examples of impulse distribut · .e shown in Fig. 14, applicable to buffer plates with minimum thicknesses h_0 of 1/4, 3/8, and 1/2 inch and to a flyer plate thickness of 25 mils (Fig. 11 was used to obtain the curves in Fig. 14). The impulses are normalized by the values of the peak impulses. Other data such as the outer and inner radii are shown in the figure. It can be seen that in these examples the impulse varies approximately as cos θ for θ in the ranges $-60^\circ < \theta < 60^\circ$, $-65^\circ < \theta < 65^\circ$, and $-75^\circ < \theta < 75^\circ$ for h_0 equal to 1/2, 3/8, and 1/4 inch respectively; these ranges cover the main regions of interest in test rings. Attenuators placed over the outside surfaces of the buffer plates and outside the above regions reduce the flyer plate velocities significantly so that a cosine distribution can be approximated around the entire buffer.

e. Contact Velocity of Flyer Plate

As the detonation front travels at the detonation velocity around the outside of the buffer plate, the flyer plate is spalled off the inner surface of the buffer plate. Because of the time taken for the stress pulse to traverse the buffer and flyer plates and back to the interface, the point of departure of flyer and buffer lags behind the detonation front. For a buffer plate of constant thickness, this point of departure travels at the detonation velocity in the circumferential direction. Since the thickness of the buffer plate beneath the detonation front is decreasing in the first quadrant of travel and increasing in the second, the point of departure travels circumferentially at a velocity slightly greater than the detonation velocity in the first quadrant and slightly less than the detonation velocity in the second. In establishing the circumferential velocity of the point of contact of the flyer plate with the target ring this slight variation is neglected.

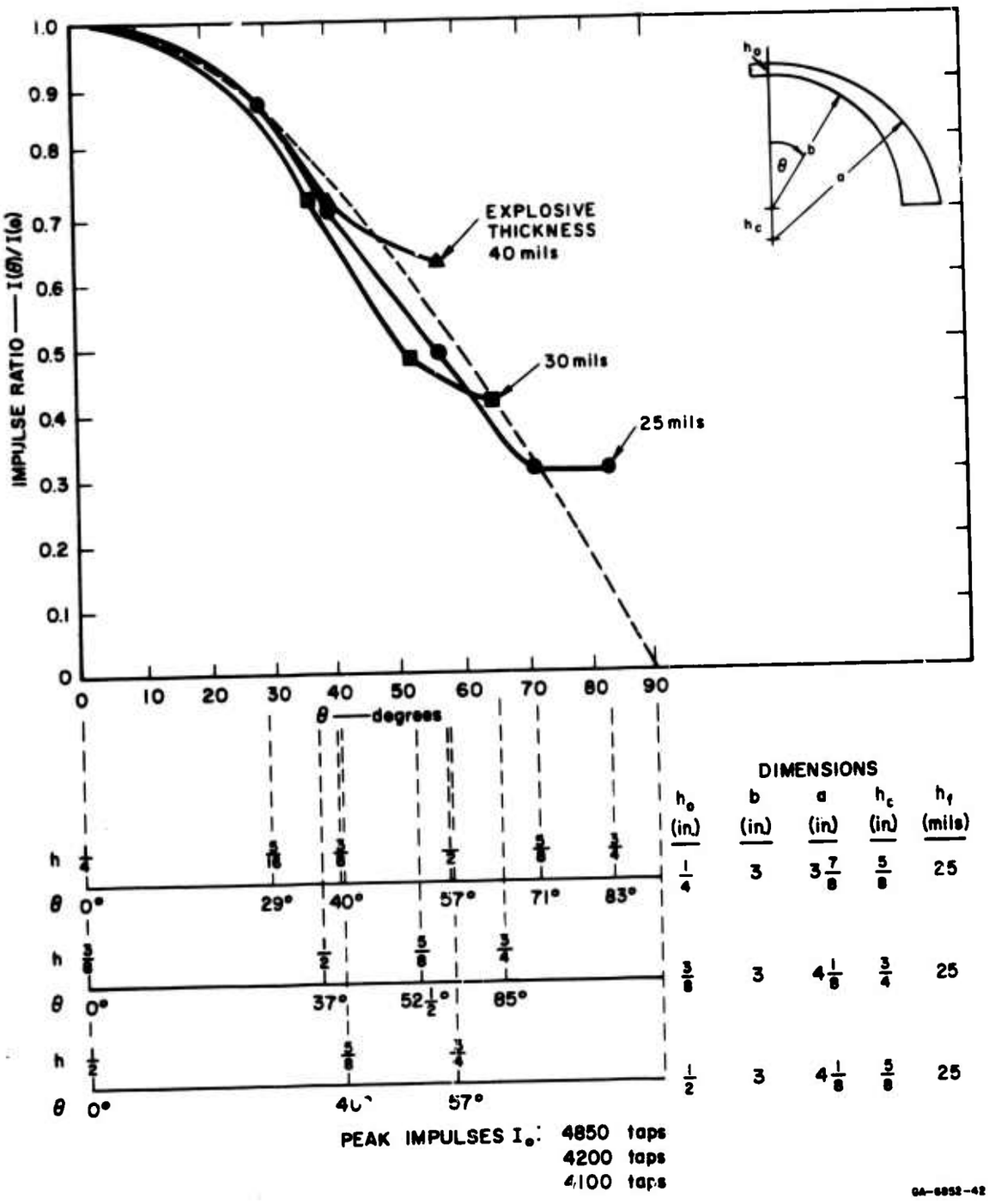

FIG. 14 IMPULSE DISTRIBUTIONS FOR 25-MIL THICK FLYERS

Figure 15 shows a simplified version of the buffer-flyer-target geometry. The angular coordinates of the detonation front and of the point of contact of the flyer and target are θ_d and θ_c (the time delay caused by plate thickness has been neglected in the geometrical representation of Fig. 15). The curve representing the radially inward displacement of the flyer at each instant (at each value of θ_d) is $w(\theta, \theta_d) = v(\theta)\Delta t$, where $v(\theta)$ is the required velocity distribution and Δt is the time during which the point on the flyer at coordinate θ has been in motion. This time is $\Delta t = a(\theta_d - \theta)/V$. Thus for a required velocity of $v(\theta) = v_o \cos\theta$ the flyer displacement is

$$w(\theta, \theta_d) = (v_o a/V)(\theta_d - \theta) \cos\theta$$

For convenience, this displacement is rendered dimensionless by dividing by the flyer displacement at section $\theta = 0$ when the detonation front has traveled around two quadrants, that is, $\theta_d = \pi/2$. In dimensionless terms then, the displacement expression becomes

$$w(\theta, \theta_d)/(\pi a v_o/2V) = (2/\pi)(\theta_d - \theta) \cos\theta \qquad (1)$$

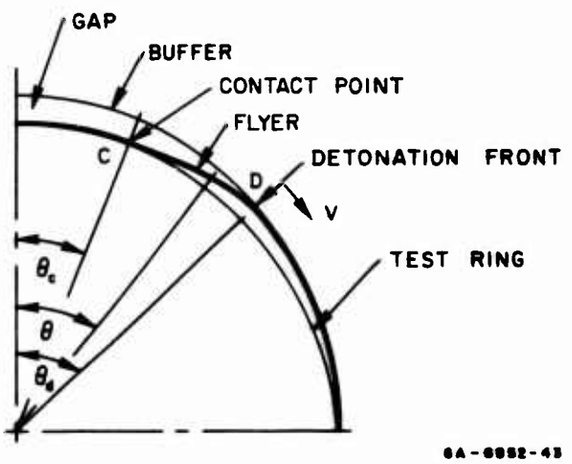

FIG. 15 SIMPLIFIED BUFFER-FLYER-TARGET GEOMETRY

If the initial gap h_g between flyer and target surface is chosen to vary as $\cos\theta$ it may be represented in the dimensionless form

$$h_g(\theta)/(\pi a v_o/2V) = k\cos\theta \qquad (2)$$

where k is a constant giving the gap amplitude.

The required dependency of the contact coordinate θ_c upon the detonation velocity coordinate θ_d, found by equating (1) and (2), is simply the linear relationship

$$\theta_c = \theta_d - k\pi/2$$

indicating that the contact velocity equals the detonation velocity. To obtain the constant lag angle $\theta_d - \theta_c = k\pi/2$ for a few practical cases, consider the data $a = 3.0$ inches, $h_g(0) = 0.090$ inch (maximum gap), $V = 7.2$ mm/μsec, and maximum flyer velocities of $v_o = 0.1$, 0.2, and 0.3 mm/μsec. For these values of v_o, the data result in the k values 1.365, 0.6825, and 0.455.

In practice, it is simple to provide a gap varying as $\cos\theta$. If the inside radius of the flyer is the same as the outer radius of the test ring and the centers are located a distance $h_g(0)$ apart, then as long as the ratio $h_g(0)/\text{radius}$ is small and symmetry maintained, the gap is approximately $h_g(\theta) = h_g(0)\cos\theta$.

f. Pulse Shape Prediction

An indication of the pulse shape at the flyer-target interface is readily obtained if it is assumed that both flyer plate and heat shield materials behave elastically, that the geometry is planar instead of cylindrical, and that the impact is simultaneous instead of running. Thus one-dimensional plane strain conditions are substituted for the actual conditions.

As a relevant example, consider an aluminum flyer plate of thickness $h_f = 25$ mils, density $\rho_f = 2.7$ g/cm^3, and dilational velocity $c_{df} = 6.3$ mm/μsec impacting at velocity $v = 0.2$ mm/μsec, a carbon phenolic layer

of thickness h_t = 200 mils, density ρ_t = 1.5 g/cm^3, and dilational velocity c_{dt} = 4.2 mm/μsec. Plane elastic impact immediately produces a peak pressure of

$$p = (\rho c_d)_t (\rho c_d)_f v/[(\rho c_d)_t + (\rho c_d)_f]$$

which, upon substitution of the above data gives p = 9.2 kbar. The remaining stress wave calculations for this example are exhibited in Fig. 16. Figure 16a is the space-time (x-t) diagram and shows that 10 reverberations occur in the flyer plate before the reflection from the rear surface of the carbon phenolic layer arrives at the interface. During this time pressure and particle velocity at the interface decrease in the manner shown in Fig. 16b. From Fig. 16b and the knowledge that the transit time of a wave in the aluminum flyer is 0.1 μsec, the pressure-time diagram of Fig. 16c is constructed. The pressure has fallen to less than 7 percent of its peak value in less than 0.65 μsec.

4. RING TESTS

Upon completion of development, the technique was used to apply impulsive loads to five rings. Three of the rings were a composite consisting of a base ring of 6061-T6 Aluminum alloy, 50 mils thick with a 6-inch outside diameter, bonded with a 30-mil-thick layer of Epon 934* (hard bond) to a cover ring of 200-mil-thick silica phenolic. Each of these three rings was 3/4 inch wide. In each case the buffer plate was 1/4 inch thick at the center and the sheet explosive was 25 mils thick. In the first two tests flyer plates 25 mils thick and 3/4 inch wide were used; the peak impulse, from Fig. 11, was therefore about 4850 taps and the distribution of impulse approximating cos θ corresponds to the appropriate curve in Fig. 14. The third test was similar except that flyer plate thickness was 50 mils; the peak impulse, from Fig. 12, was therefore about 7800 taps and the distribution was approximately like cos θ. In all three cases visible debonding (symmetrical in θ) occurred

*Trademark, Shell Chemical Company.

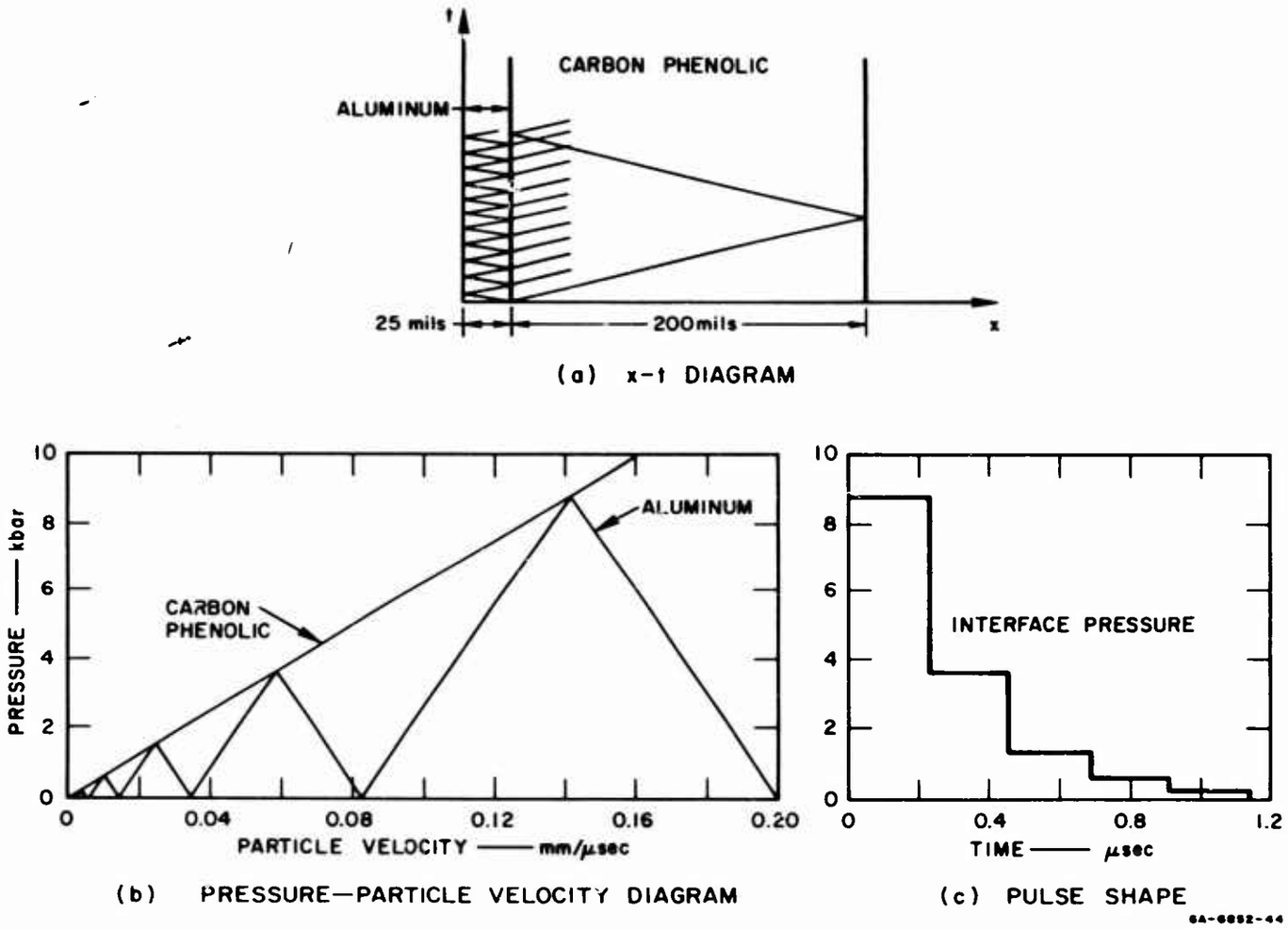

FIG. 16 GRAPHICAL CONSTRUCTION OF PULSE SHAPE AT FLYER-HEAT SHIELD INTERFACE

and the structural damage was negligible, although in the third test plastic buckling of the base ring was incipient. Also, the first two tests produced identical results.

Two Narmco-wrap* rings were also tested with the flyer plate technique. Each ring had an outside diameter of 5-3/4 inches, a width of 1-1/2 inches, and a thickness of 3/8 inch. The construction is based on an integrated heat shield concept with an orthogonal fiber (Thornel 25**) arrangement in the circumferential and axial directions of the structural inner layer, and with 15-mil-diameter mild steel staples in the radial direction. The outer heat shield layer is composed of tape-wrapped carbon fabric (CCA-1) in a resin system (PBI or polybenzmidizole). In these two tests, the buffer plate was 3/8 inch thick at the center and the flyer plates were 25 mils thick and 1-1/2 inches wide. In the first test, the explosive thickness was 30 mils which, according to the calibration curve in Fig. 11, provided a peak impulse of 4100 taps and an impulse distribution corresponding to the appropriate curve in Fig. 14. The resulting damage was slight, as can be seen in the ring photographs of Figs. 17a and b. A small strip of the heat shield layer was removed from one edge because of the tape wrapping angle. It should be noted that this type of damage would not occur in a cylindrical shell because of the special construction that is incorporated over supports. The second test was similar except that the explosive was 40 mils thick which, according to the calibration curve in Fig. 11, provided a peak impulse of 5250 taps and an impulse distribution corresponding to the appropriate curve in Fig. 14. The resulting damage is shown in Figs. 17c and d. Again an edge strip of heat shield material has been removed which, as mentioned above, is not very significant. The main damage is the extensive cracking in the region below the peak impulse (marked by a zero in the figure, indicating $\theta = 0$). Also, back from the front edge, two small pieces of heat shield have been removed, forming a surface cavity.

---

*Manufactured by Whittaker Corporation, Narmco Research and Development Division, 3540 Aero Court, San Diego, California 92123.

**Trademark, Union Carbide Corporation.

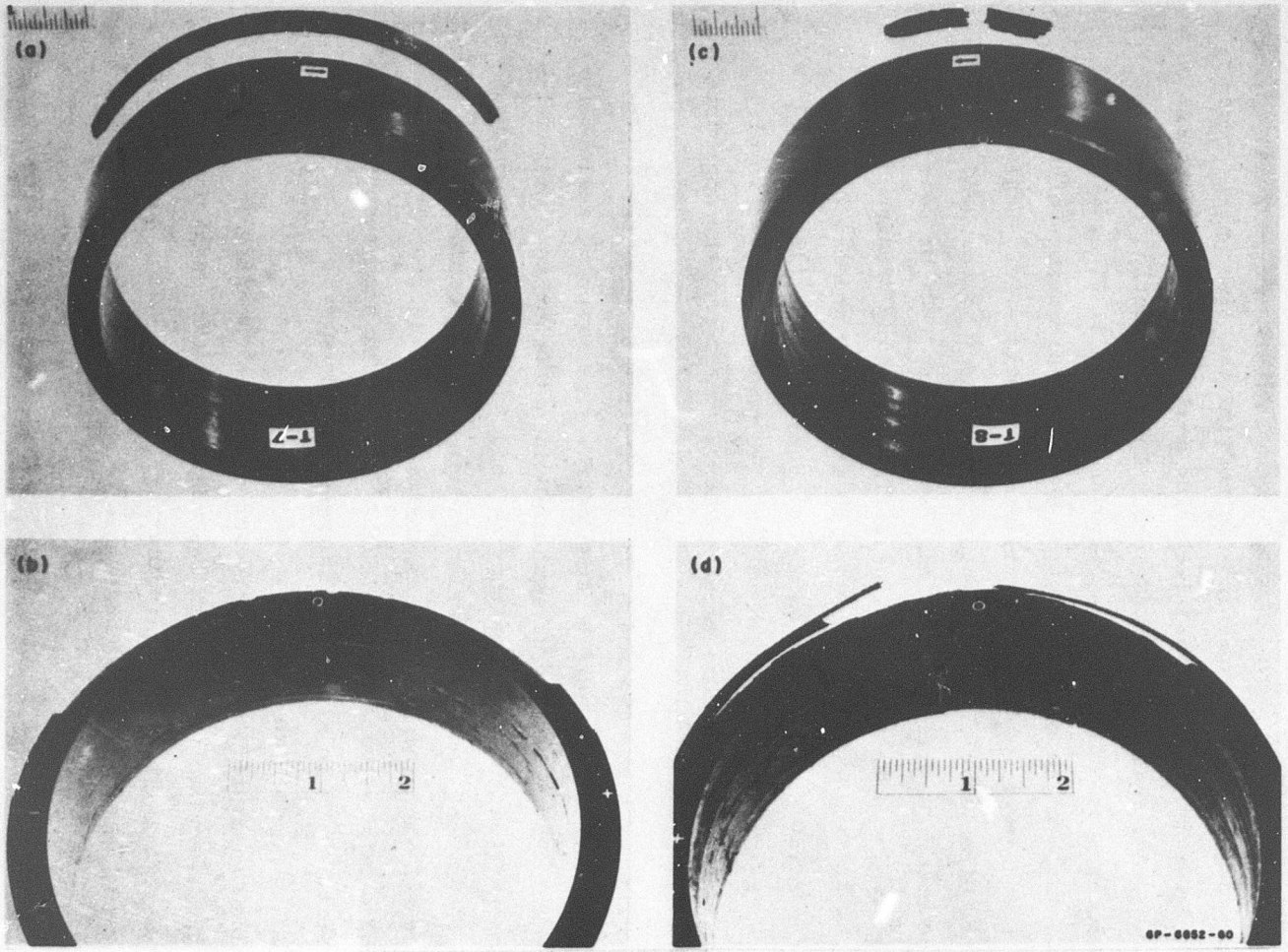

FIG. 17 TWO NARMCO-WRAP RINGS AFTER IMPACT WITH 25-MIL-THICK FLYERS.
(a) and (b) Damage from impulse with 4100 taps peak.
(c) and (d) Damage from impulse with 5250 taps peak.

SECTION III

A SPRING-MASS IMPULSE GAGE

1. INTRODUCTION

An important factor in reentry vehicle vulnerability and lethality analysis is the impulse imparted to materials by nuclear weapons. In underground nuclear tests impulses are measured with both active and passive impulse gages. Passive impulse gages are included because they inexpensively provide valuable data to supplement data from active gages. They have the advantages of simple construction and ease of installation. Passive gages can record impulses imparted to one-dimensional samples without significantly affecting the response of the samples.

This section describes a spring-mass impulse gage that was developed to overcome the disadvantages of existing passive impulse gages and that incorporates a recording device for separating deflections caused by impulses from those caused by later extraneous loads such as hurricanes, bulkhead shock, and ground motion. This description will follow a review of five types of passive impulse gages that have been used in underground nuclear tests, which will provide a basis of comparison.

2. REVIEW OF PASSIVE IMPULSE GAGES

This review is taken from notes* on a meeting held at Stanford Research Institute on October 11, 1967.

a. Description of Gages

Schematic drawings of the five gages considered are given in Fig. 18. These gages are known as the indenter, foam, MRI,** flyer plate, and beam

*"Review of Passive Impulse Gages" by G. R. Abrahamson, December 19, 1967.

**Mechanics Research, Inc.

gages. All of the gages operate by absorbing the kinetic energy of a rigid mass in permanent deformation of a recording element.

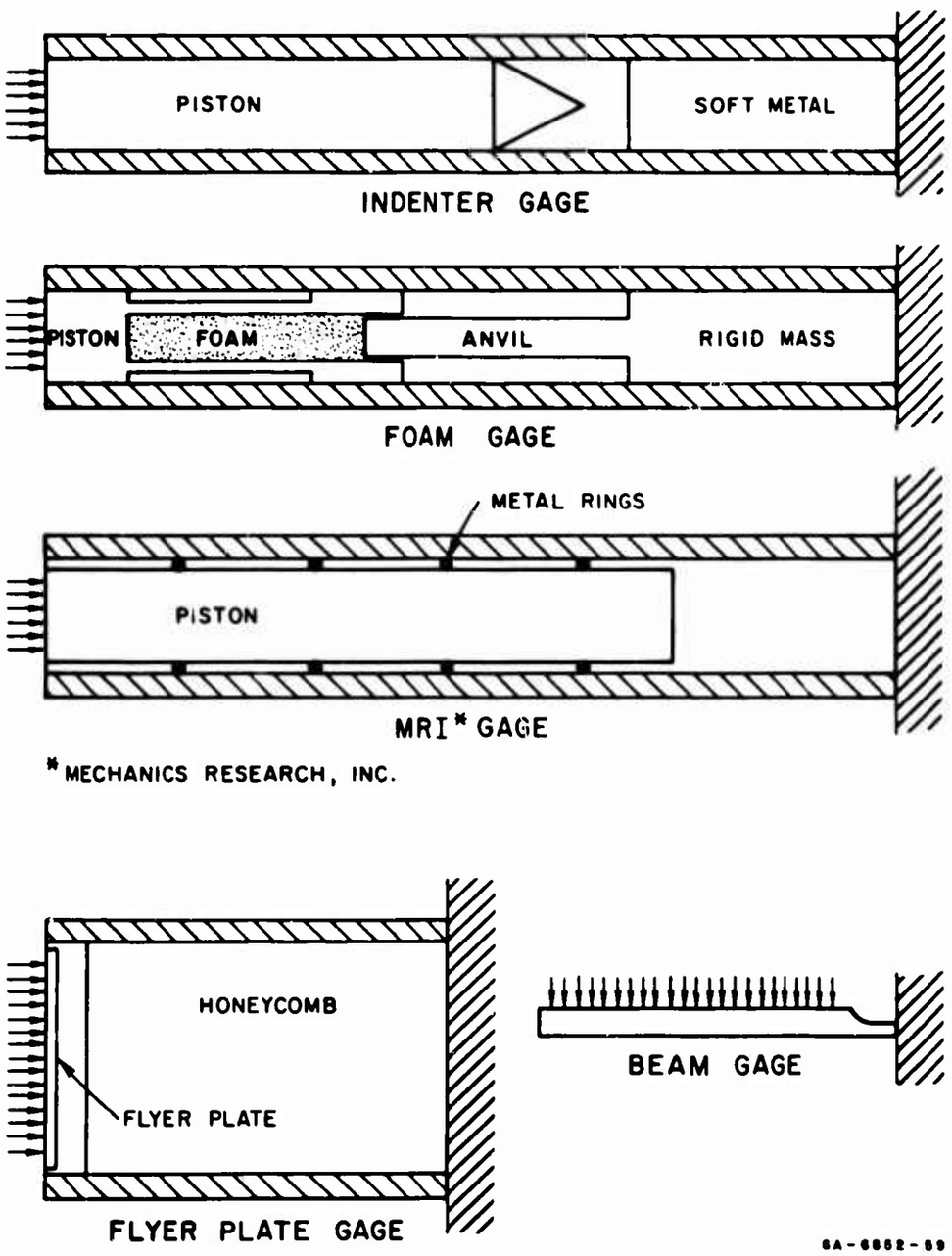

FIG. 18 DIAGRAMS OF EXISTING PASSIVE IMPULSE GAGES

The first three gages convert the impulse into kinetic energy of a massive piston. In the indenter gage, the kinetic energy of the piston is absorbed by having the piston (pointed end) impact a block of metal, such as soft copper. In the foam gage, the kinetic energy is absorbed by having the piston (flat end) crush a rigid plastic foam. In the MRI gage, which is reversible and reusable, the energy is absorbed by deformation of metal rings.

The flyer plate gage converts the impulse into kinetic energy of a thin plate (hence the energy is much greater than with the heavier pistons) which in turn is absorbed by crushing aluminum honeycomb. The beam gage converts the impulse into kinetic energy of a cantilever which in turn is absorbed in plastic bending near the support.

b. Extraneous Loads

The first weapon-induced extraneous effect is blowoff from materials adjacent to a gage. Pressure from the gases formed cause deflection of a gage mass additional to that caused by the impulse being measured.

"Hurricane" refers to the wind that results from gases rushing into the weapon end of the steel pipe containing the underground experiment when the pipe ruptures. Hurricane loads differ from those from adjacent blowoff in that they arrive much later ($\sim$ 100 msec) and they last much longer. Again, additional deflections can occur.

The third extraneous effect is bulkhead shock caused by the impulse imparted to the bulkhead to which the gages are attached.

Ground motion produces extraneous effects by shaking the pipe. This shaking causes acceleration of the bulkheads and creates inertial loads in the impulse gages.

The final extraneous effect is anomalous heating.

c. Gage Characteristics

Table I gives the basic characteristics of the five gages. The range factor 2 listed in column five means that a gage designed for an impulse I can record with the same accuracy between $2I$ and $I/2$ (provided the impulse $I/2$ exceeds the minimum level).

Table I

BASIC CHARACTERISTICS OF EXISTING PASSIVE IMPULSE GAGES

Gage	Repro-ducibility (%)*	Impulse Range		Range Factor	Deflection (in.)**	Area ($in.^2$)	Remarks
		Min. (taps)	Max. (taps)				
Indenter	5	200	$>10^5$	†	1/8	1	††
Foam	10	1000	$>10^5$	2	1	1	†† Elastic rebound
MRI	5	100	$>10^5$	2	1	1	
Flyer Plate	5-10	1000	$>10^5$	2	1/2	2	††
Beam	10	100	$>10^5$	2	1	1	

*In cassette, under laboratory conditions.
**Normal deflection range.
†Single gage extends over entire range.
††Recording element in path of radiation

Table II gives the field characteristics of the gages in relative terms. The sensitivities of indenter and foam gages to adjacent blowoff effects are low to moderate because they can be ventilated. The sensitivity of the beam gage to adjacent blowoff is low because it is well vented.

The piston of the indenter gage can be removed from the path of the hurricane by allowing it to drop. However, this exposes the recording surface. The sensitivities of the foam gage and flyer plate gage to hurricane are greater than to adjacent blowoff because, if the piston or plate has rebounded a significant distance, the hurricane can accelerate the piston or plate until it reaches the recording element. In the MRI gage, the piston is not free to accelerate, hence its sensitivity to hurricane is about the same as adjacent blowoff. The beam gage is probably less sensitive to hurricane than to adjacent blowoff because, as it deflects, it turns parallel to the pipe.

Table II

FIELD CHARACTERISTICS OF EXISTING PASSIVE IMPULSE GAGES

Gage	Sensitivity to Preshot Mishandling	Preshot Check		Sensitivity to Extraneous Effects					Data Recovery	
		Rigid Mass	Recording Element	Adjacent Blowoff	Hurricane	Bulkhead Shock	Ground Motion	Anomalous Heating	Tunnel	Sensitivity to Mishandling
Indenter	low*	easy	difficult	low-mod	moderate	high	moderate	low	maybe	low*
Foam	low*	easy	easy	moderate	mod-high	moderate	moderate	high	yes	low*
MRI	low*	easy	easy	mod-high	mod-high	moderate	moderate	low	yes	low*
Flyer Plate	high	easy	difficult	moderate	mod-high	low	low	low	maybe	low
Beam	moderate	easy	easy	low	low	moderate	moderate	low	yes	moderate

*Assuming use of setscrews to hold piston.

The sensitivity of the indenter gage to bulkhead shock is high because the piston travel is small and even small amplitude vibrations of the bulkhead may cause the piston to bounce back and forth. However, if the piston has dropped, this effect will not alter the recording. The foam, MRI, and beam gages are less sensitive to bulkhead shock because they have larger deflections and hence can generally sustain greater bulkhead motion without being affected significantly. The sensitivity of the flyer plate gage to bulkhead shock is low because of the low mass of the plate.

Because ground motion loads are probably less intense than those from bulkhead shock, but last longer, the sensitivity of the indenter gage will probably be somewhat less than to bulkhead shock, and the sensitivities of the other gages will be about the same as to bulkhead shock.

All of the gages are insensitive to such heating up to the softening point of metals, except for the foam gage which is affected when the temperature reaches the decomposition temperature of the foam.

The foam, MRI, and beam gages allow the deflection to be measured before removal, and the indenter and flyer plate gages could be modified to permit this.

The sensitivity of the beam gage is more sensitive to mishandling than the other gages.

b. Discussion

The major difficulties with passive impulse gages stem from the extraneous weapon-induced effects. No attempt has been made to determine the magnitudes of the various effects in order to ascertain which are the most important for passive impulse gage design. However, methods for alleviating the various effects were considered.

The effects of adjacent blowoff can be minimized by venting so that the net load developed is reduced, or by putting the gage in a container (such as a pipe) which keeps the gases away from the loading surface. The effects of bulkhead shock can be minimized by ordinary shock mounting methods.

There is no apparent way to reduce the effects of hurricane or ground motion by improved gage design. However, because these effects are widely separated in time from the primary load, the effects of the primary and extraneous loads may be differentiated with a simple timing scheme. A timing scheme appears to be quite feasible for the foam, MRI, and beam gages, all of which have heavy, rigid masses and give large deflections. It appears to be difficult to devise a timing scheme for the indenter gage because of the small deflections, or for the flyer plate gage because of the small mass of the plate. The idea of incorporating a recording scheme makes attractive the possibility of using a mechanical spring as the energy absorber. A spring-mass gage has definite advantages because it permits nondestructive calibration of the recording element, as with the MRI gage.

Two rankings of the gages were made, the first without a timing scheme for separating the primary and extraneous loads, and the second with such a timing scheme. These rankings are given in Table III.

Table IV gives a summary of past usage of passive impulse gages.

Table III

RANKINGS OF EXISTING PASSIVE IMPULSE GAGES

Impulse Range (taps)	Without Timing Scheme	With Timing Scheme
100-1000	(1) beam (2) indenter (3) MRI	(1) beam (2) MRI (3) indenter
> 1000	(1) beam (2) flyer plate (3) MRI (4) foam (5) indenter	(1) beam (2) MRI (3) foam (4) flyer plate (5) indenter

Table IV

PAST USAGE OF PASSIVE IMPULSE GAGES

Gage*	Underground Test
Indenter	Marshmallow (AFWL/ASE) Fishbowl (AFML/ASE), (AFML/ARA) Double Play (BSD/Avco) Midi Mist (BSD/Avco) Gum Drop (AFWL) Dorsal Fin (AFWL/Avco)
Foam	Dorsal Fin (AFWL/SRI)
MRI	Dorsal Fin (AFWL/SRI
Flyer Plate	Double Play (Sandia, Livermore) Midi Mist (Sandia, Livermore) Door Mist (Sandia, Livermore) Hupmobile (Sandia, Livermore) Dorsal Fin (Sandia, Livermore)
Beam	Double Play (AFWL/SRI) Door Mist (Sandia, Livermore) Dorsal Fin (AFWL/SRI)

*See the list of References at the end of this report for related key documents (Refs. 2-12).

3. SPRING-MASS GAGE

a. Description

In the light of the foregoing review a spring-mass gage has been developed which incorporates a recording device for separating deflections caused by the impulse from those caused by extraneous loads such as ground shock, bulkhead shock, and hurricanes.

A schematic drawing of the gage is shown in Fig. 19. The impulse imparted to the exposed end of the steel piston is converted into momentum and the corresponding kinetic energy of the piston is ultimately absorbed as elastic strain energy in the steel helical spring. Once the piston comes to rest, it automatically locks in position to prevent rebound but not to prevent further possible deflection from extraneous loading. The recording device described below makes use of this one-way motion. Elimination of rebound also prevents further damage to a sample mounted on the front face of a piston.

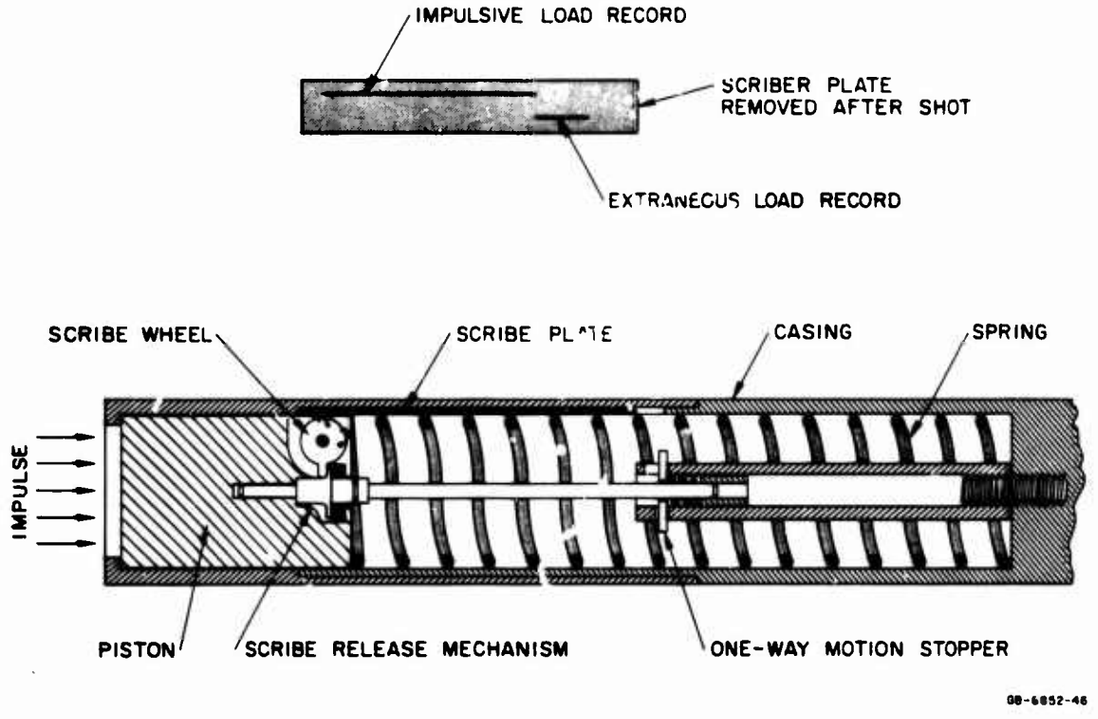

FIG. 19 DIAGRAM OF SPRING-MASS PASSIVE IMPULSE GAGE SHOWING RECORD

A device to record travel is attached at the rear of the piston. This device is essentially a scriber mounted radially on one side of a small spring-loaded wheel so that it bears against a specially coated foil fixed to the inside of the gage casing. A straight line is scribed on the foil during piston motion. When motion ceases, the scriber is automatically disengaged from the recording surface by rotation of the small supporting wheel while a second radially oriented scriber mounted on the opposite side of the wheel is brought to bear against the recording surface. The values of the piston mass and spring stiffness are chosen to keep the fundamental response time of the gage well below the interval between the arrival times of the impulse and the extraneous loading. Upon arrival of the extraneous loading, the piston may be further deflected and its additional travel recorded by the second scriber. Thus the record will consist of two straight lines set off from one another as shown in Fig. 19, and the final deflection of the piston, locked in position, checks the sum of the lengths of the two straight lines.

b. Current Stage of Development

The spring-mass gage shown in Fig. 20 was constructed to put the above design to test. Design details are contained in Appendix I (the overall dimensions are 1 inch for the diameter and 8 inches for the length). The gage was subjected four times to impulsive loading from detonating sheet explosive on the exposed piston surface. In each experiment the recording and locking devices operated satisfactorily and the impulse readings were duplicated at levels of 6300 and 11,600 taps. The gage was not subjected to a second pulse to represent extraneous loading, but the scribe mechanism was consistently in the correct position at the end of the impulsively induced motion so that additional deflections would have been recorded.

Later, the larger spring-mass gage shown in Fig. 21 was constructed to measure impulses in excess of 40 ktaps. Design details are contained in Appendix II (the overall dimensions are 2-1/2 inches for the diameter and 13 inches for the length). In each of three identical impulsive loading tests, the recording and locking devices operated satisfactorily

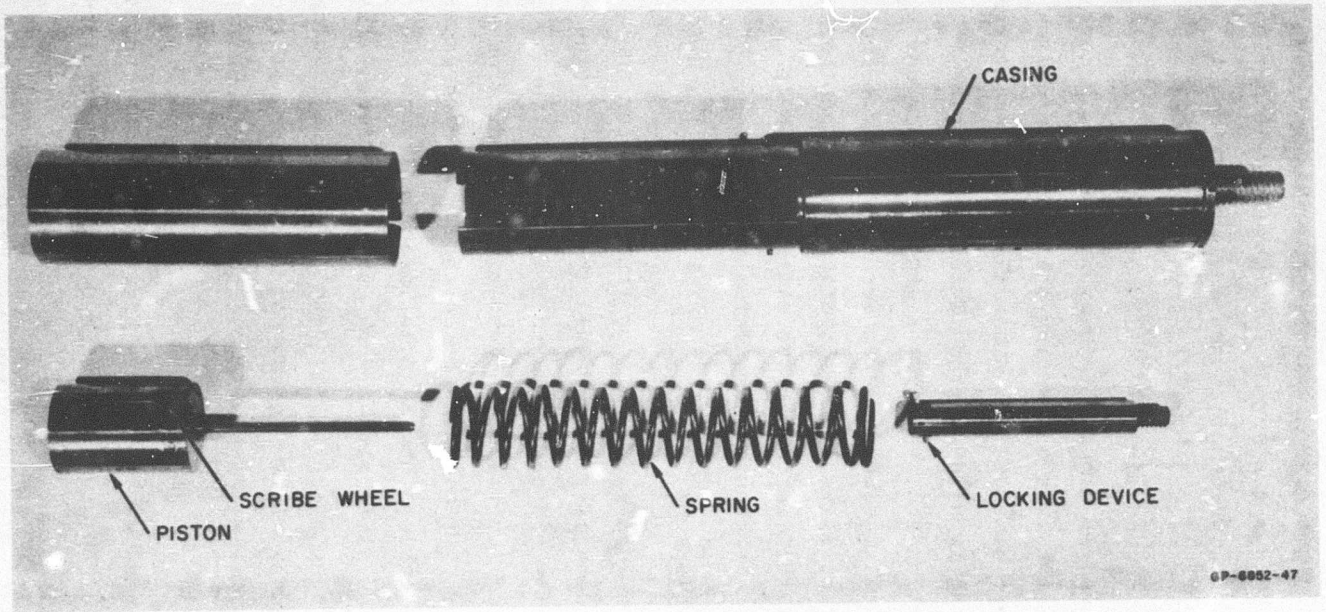

FIG. 20 15-ktap SPRING-MASS PASSIVE IMPULSE GAGE

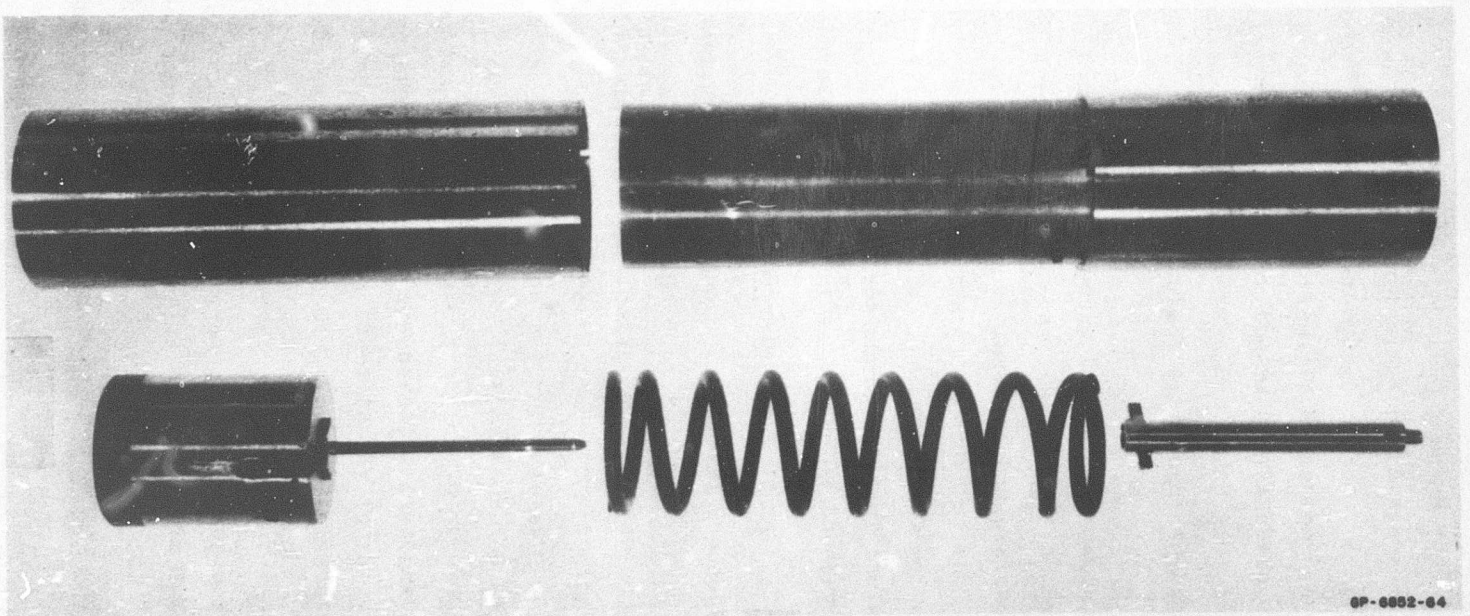

FIG. 21 40-ktap SPRING-MASS PASSIVE IMPULSE GAGE

and the impulse reading was reproduced at 29,000 taps. In each test the scribe mechanism was in the correct position for recording any deflection caused by additional pulse loading.

c. Features

The spring-mass gage has the following desirable features:

1. Ability to record impulses with reduced susceptibility to extraneous loading.

2. Possibility of calibration before and after underground nuclear tests.

3. Accurate recording over a wide range of loadings (impulse proportional to piston deflection).

4. Reproducibility.

5. Immunity to high temperatures.

6. Ease of handling (robust, almost foolproof, and easy to install).

7. Production of permanent record that can be easily removed from the gage.

8. Absence of piston rebound and possible further damage to attached samples.

d. Future Work to Complete Gage Development

Work required to complete the development of the spring-mass gage includes:

1. An experimental and theoretical determination of a best choice of piston mass and spring constant corresponding to the impulse range to be covered by a gage.

2. Dynamic testing, such as impulsive loading followed by blast loading or inertial loading to simulate conditions experienced in underground tests.

3. Sufficient pulse load testing to establish degree of repeatability over a wide range of impulses.

4. Design refinements to improve the operation and recording system of the gages.

5. Design and testing of gages having samples attached to the front faces of the pistons.

Simulation of impulsive loading followed by blast loading occurring in underground tests can be carried out with sheet explosive in direct contact with the piston face and a high-explosive sphere located at an appropriate distance from the piston face and on the gage axis. Detonation times can be arranged to allow the blast wave to strike the piston approximately 100 msec after the impulsive loading from the sheet explosive. Simulation of ground and bulkhead motion can be carried out by subjecting a gage to high accelerations.

This page intentionally left blank.

REFERENCES

1. Lindberg, H. E.; Gates, R. W.; Baer, M. J.; Simulation and Structural Effects of Sharp Pulses, Vol. II, Stanford Research Institute Final Report, June 15, 1964.

Indenter Gage

2. Harmon, N., et al.; Passive Momentum Experiment in Shot Marshmallow (U), POR-1852 (WT-1852), Project 833.4, May 1, 1964 (SRD).

3. Gillespie, C. M.; Wing, P. G.; Operation Dominic, Fish Bowl Series, (U), POR-2038 (WT-2038), Project 8B, December 15, 1965 (SRD).

4. Wing, P. G., et al.; Final Report on Recoverable Instrument Design and Analysis for DASA Project 837 (U), SWC-OS-21375

5. Anderson, O. A., et al.; Shots Blue Gill and King Fish, Vol. II, (U), POR-2037 (WT-2037), Project 8A.3, March 29, 1965 (SRD).

6. Dabrowski, S. A.; Double Play Project 8.01 (U)," Avco Corporation Project Officers Report, AVMSD-0611-67-RR, September 1967 (SRD)

7. Kowalczyk, F. S.; Pretest Report for Effects on Material Specimens in Door Mist (U), Avco Corporation AVSSD-0253-67-CR, July 3, 1967 (SRD)

8. Kowalczyk, F. S.; Pretest Report for Effects on Material Specimens in Dorsal Fin (U), Avco Corporation AVSSD-0383-67-CR, September 25, 1967 (SRD).

Foam Gage

9. Samuelsen, G. S.; Abrahamson, G. R.; SRI Shock and Structural Effects Experiment (U), Stanford Research Institute, Pretest Report, Project 8.81, Operation Dorsal Fin, November 6, 1967 (SRD).

MRI Gage

10. Samuelsen, G. S.; Abrahamson, G. R.; SRI Shock and Structural Effects Experiment (U), Stanford Research Institute, Pretest Report, Project 8.81, Operation Dorsal Fin, November 6, 1967 (SRD).

REFERENCES (Concluded)

Flyer Plate Gage

11. Meyer, M. D.; Passive Measurement of X-Ray-Induced Blowoff Impulse (U), Sandia Corporation, Livermore, California, SCL-DR-67-45 (SRD).

Beam Gage

12. Samuelsen, G. S.; Abrahamson, G. R.; Passive Structural Experiment for Double Play (U), Stanford Research Institute, Project Officers Report, Project 8.07, March 1, 1967 (SRD).

APPENDIX I

DESIGN DETAILS OF 15-KTAP SPRING-MASS GAGE

In this appendix a gage design is presented for measuring impulses ranging from 2000 to 15,000 taps (a useful range for underground nuclear tests), and having a response time much less than 100 msec.

The simple spring-mass system representing the passive impulse gage is depicted in Fig. 22. At time t the displacement x of the piston of mass m from its initial at-rest position caused by an impulse I is

$$x = (I/\sqrt{mk})\ \sin(\sqrt{k/m}\,)t$$

where k is the spring constant. Thus the maximum piston displacement is

$$x_m = I/\sqrt{mk}$$

and the time taken for the spring to bring the piston to rest, the response time is

$$t_m = (\pi/2)\sqrt{m/k}$$

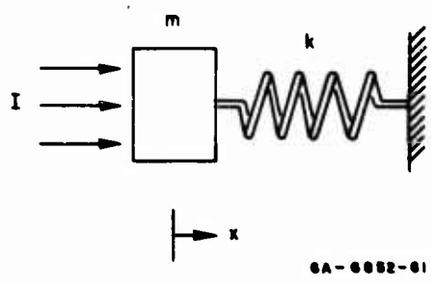

FIG. 22 SPRING-MASS SYSTEM

Design data for the spring-mass gage shown in Fig. 20 are:

Piston material:	1015 Steel
Piston weight:	m = 156 grams
Exposed diameter:	15/16 inch
Exposed area:	$A = 0.69$ in.^{2} $= 4.43$ cm^2
Spring material:	Steel music wire
Spring weight:	29.1 grams
Spring diameter:	D = 0.857 inch
Wire diameter:	d = 0.080 inch
Number of turns:	n = 14
Modulus of rigidity:	$G = 11.5 \times 10^6$ lb/in.^{2}
Spring constant:	$k = d^4G/8nD^3 = 6.65$ lb/in. $= 1.16 \times 10^6$ dynes/cm
Experimental spring constant:	k = 6.63 lb/in.
Impulse:	$I = x_m\sqrt{mk}$
Impulse/inch deflection:	$I = 34.4 \times 10^3$ dyne-sec
Impulse intensity/inch deflection:	$I_o = I/A = 7750$ taps
Maximum deflection possible:	2 inches
Maximum impulse possible:	15,500 taps
Response time:	$t_m = (\pi/2)\sqrt{m/k} = 18.2$ msec

Figure 23 shows the theoretical calibration curve for the 15-ktap impulse gage; it represents a simple linear relationship between impulse intensity and piston deflection. To keep recording accuracy it is suggested that the gage be used to measure impulses above 2000 taps, and to keep deflections below the maximum possible deflection of 2 inches, it is suggested that the gage be used to measure impulses below 15,000 taps.

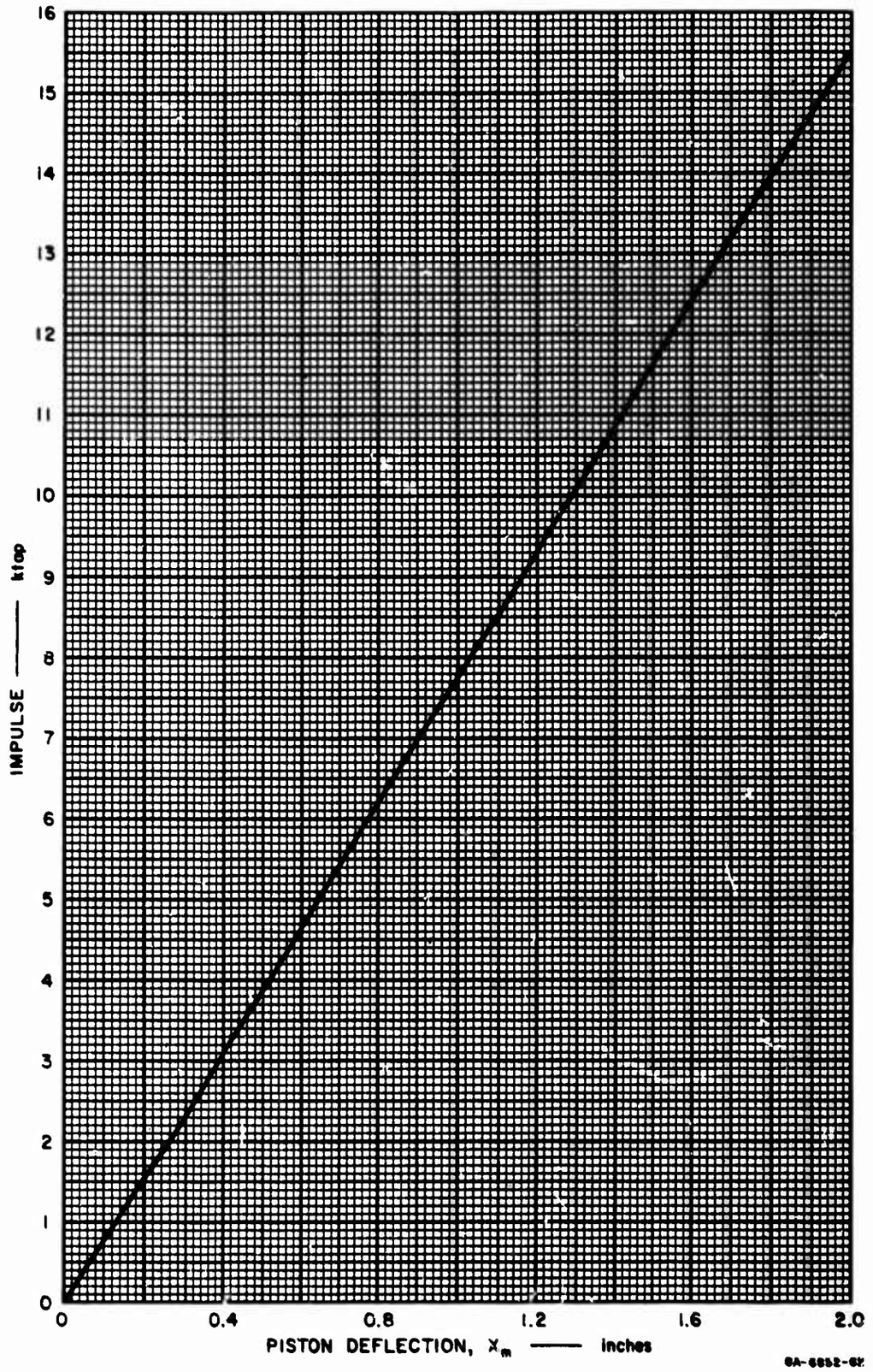

FIG. 23 THEORETICAL CALIBRATION CURVE FOR 15-ktap GAGE

This page intentionally left blank.

APPENDIX II

DESIGN DETAILS OF 40-KTAP SPRING-MASS GAGE

In this appendix a gage design is presented for measuring impulses up to 40 ktaps and having a response time much less than 100 msec.

Design data for the spring-mass gage shown in Fig. 21 are:

Piston material:	1015 Steel (4140 Steel end piece)
Piston weight:	m = 1332 grams
Exposed diameter:	1-7/8 inches
Exposed area:	$A = 2.76 \text{ in.}^2 = 17.9 \text{ cm}^2$
Spring material:	Spring steel wire (SAE 1066 oil hardened)
Spring weight:	311 grams
Spring diameter:	D = 1.838 inches
Wire diameter:	d = 0.225 inch
Number of turns:	n = 7
Modulus of rigidity:	$G = 11.5 \times 10^6 \text{ lb/in.}^2$
Spring constant:	$k = 85 \text{ lb/in.}^2 = 14.9 \times 10^6$ dynes/cm
Impulse:	$I = x_m\sqrt{mk}$
Impulse/inch deflection:	$I = 360 \times 10^3$ dyne-sec
Impulse intensity/inch deflection:	$I_o = I/A = 20$ ktap
Maximum deflection possible:	3 inches
Maximum working deflection:	2 inches
Maximum impulse (2-inch deflection):	40 ktap
Response time:	$t_m = (\pi/2)\sqrt{m/k} = 14.8$ msec

Figure 24 shows the theoretical calibration curve for the 40-ktap impulse gage; it represents a simple linear relationship between impulse intensity and piston deflection. To keep recording accuracy, it is suggested that the gage be used to measure impulses above 5000 taps. The gage is capable of measuring impulses well in excess of 40 ktap by allowing piston deflections up to 3 inches (~ 60 ktap). By lowering the spring stiffness from 85 lb/in.^{2} to 38 lb/in.^{2} an impulse of 40 ktap will deflect the piston 3 inches and the response time increases to 33.3 msec.

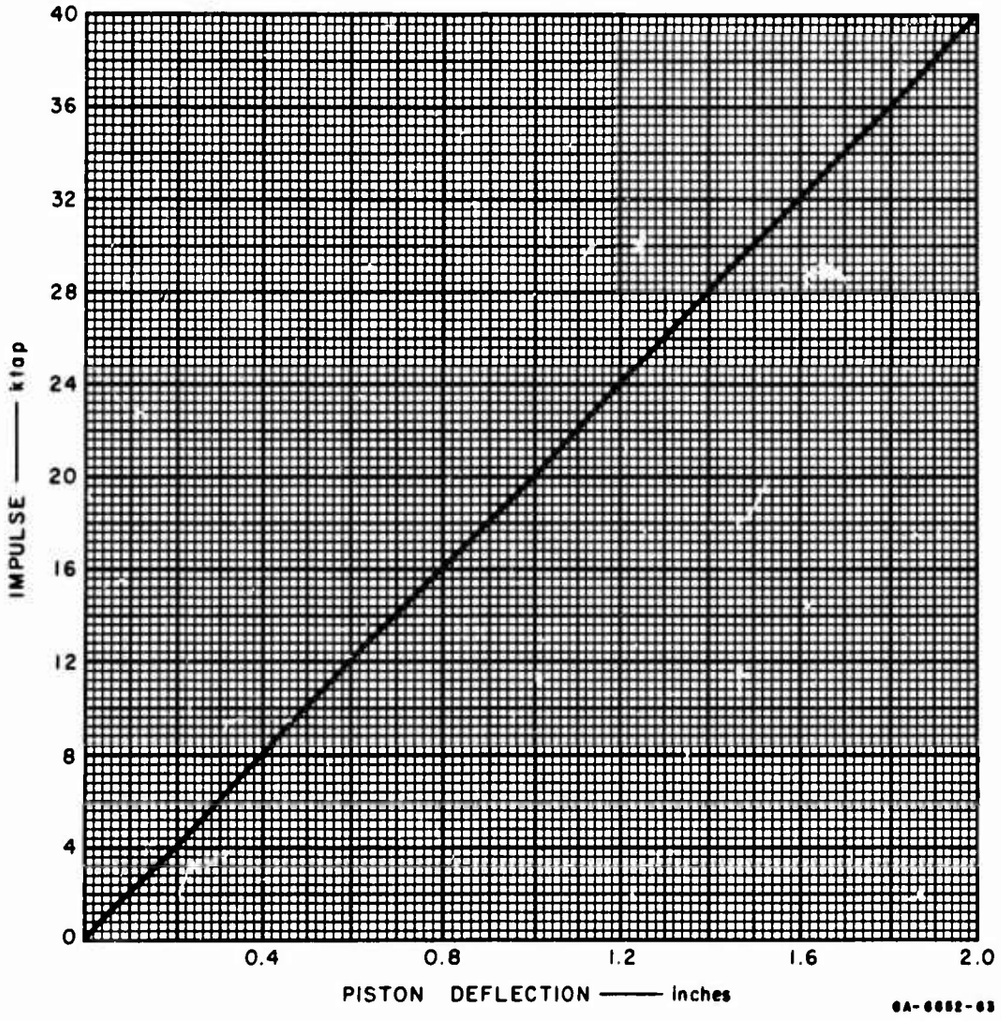

FIG. 24 THEORETICAL CALIBRATION CURVE FOR 40-ktap GAGE

UNCLASSIFIED
Security Classification

DOCUMENT CONTROL DATA - R & D

(Security classification of title, body of abstract and indexing annotation must be entered when the overall report is classified)

1. ORIGINATING ACTIVITY *(Corporate author)*
Poulter Laboratory for High Pressure Research
Stanford Research Institute
Menlo Park, California

2a. REPORT SECURITY CLASSIFICATION
Unclassified

2b. GROUP

3. REPORT TITLE
A CURVED FLYER PLATE TECHNIQUE FOR IMPULSIVE LOADING OF RINGS AND A PASSIVE IMPULSE GAGE FOR UNDERGROUND NUCLEAR TESTS

4. DESCRIPTIVE NOTES *(Type of report and inclusive dates)*
July 1968 to January 1969

5. AUTHOR(S) *(First name, middle initial, last name)*
Alexander L. Florence

6. REPORT DATE	7a. TOTAL NO. OF PAGES	7b. NO. OF REFS
June 1969	58	12

8a. CONTRACT OR GRANT NO	9a. ORIGINATOR'S REPORT NUMBER(S)
F29601-67-C-0105	AFWL-TR-68-146
b. PROJECT NO 5710	
c. Subtask 01.028	9b. OTHER REPORT NO(S) *(Any other numbers that may be assigned this report)*
d.	SRI Project PGU-6852

10. DISTRIBUTION STATEMENT This document is subject to special export controls and each transmittal to foreign governments or foreign nationals may be made only with prior approval of AFWL (WLRP), Kirtland AFB, NM 87117. Distribution is limited because of the technology discussed in the report.

11. SUPPLEMENTARY NOTES	12. SPONSORING MILITARY ACTIVITY
	AFWL (WLRP) Kirtland AFB, NM 87117

13. ABSTRACT

(Distribution Limitation Statement No. 2)

A technique has been developed for impulsive loading of rings. It consists of spalling a thin, curved flyer plate from the inner surface of a curved buffer plate by the pressure pulse from sheet explosive on an outer surface. The flyer plate travels radially inward a short distance before impacting a test ring. A $\cos\theta$ ($-\pi/2 < \theta < \pi/2$) circumferential distribution of impulse is achieved by an appropriate circumferential variation in buffer thickness. The technique is suitable for peak impulses up to 8000 taps. (Above this impulse level sheet explosive in direct contact with test rings provides the required simulation.) Impulse calibration data is presented for 25-mil and 50-mil-thick flyer plates of 6061-T6 aluminum. Tests indicate that the technique is suitable for aboveground screening of hardened materials. A passive impulse gage has been developed for use in underground nuclear tests. It consists of a piston and restraining spring and incorporates a recording device for separating the piston deflection due to the impulsive load and the deflection due to later arriving extraneous loads.

DD FORM 1 NOV 65 1473

UNCLASSIFIED
Security Classification

14 KEY WORDS	LINK A		LINK B		LINK C	
	ROLE	WT	ROLE	WT	ROLE	WT
Passive impulse gage Structural response simulation techniques						